A Linear Immersed Finite Element Space Defined by Actual Interface Curve on Triangular Meshes

Ruchi Guo

Thesis submitted to the Faculty of the
Virginia Polytechnic Institute and State University
in partial fulfillment of the requirements for the degree of

Master of Science
in
Mathematics

Tao Lin, Chair
Slimane Adjerid
Christopher A. Beattie

March 21, 2017
Blacksburg, Virginia

Keywords: Elliptic Interface Problems, Immersed Finite Element, Linear Finite Element, Interpolation Error Analysis, Interface Independent Mesh

A Linear Immersed Finite Element Space Defined by Actual Interface Curve on Triangular Meshes

Ruchi Guo

(ABSTRACT)

In this thesis, we develop the a new immersed finite element(IFE) space formed by piecewise linear polynomials defined on sub-elements cut by the actual interface curve for solving elliptic interface problems on interface independent meshes. A group of geometric identities and estimates on interface elements are derived. Based on these geometric identities and estimates, we establish a multi-point Taylor expansion of the true solutions and show the estimates for the second order terms in the expansion. Then, we construct the local IFE spaces by imposing the weak jump conditions and nodal value conditions on the piecewise polynomials. The unisolvence of the IFE shape functions is proven by the invertibility of the well-known Sherman-Morrison system. Furthermore we derive a group of fundamental identities about the IFE shape functions, which show that the two polynomial components in an IFE shape function are highly related. Finally we employ these fundamental identities and the multi-point Taylor expansion to derive the estimates for IFE interpolation errors in L^2 and semi-H^1 norms.

A Linear Immersed Finite Element Space Defined by Actual Interface Curve on Triangular Meshes

Ruchi Guo

GENERAL AUDIENCE ABSTRACT

Interface problems occur in many mathematical models in science and engineering that are posed on domains consisting of multiple materials. In general, materials in a modeling domain have different physical or chemical properties; thus, the transmission behaviors across the interface between different materials must be considered. Partial differential equations (PDEs) are often employed in these models and their coefficients are usually discontinuous across the material interface. This leads to the so called interface problems for the involved PDEs whose solutions are usually not smooth across the interface, and this non-smoothness is an obstacle for mathematical analysis and numerical computation. In this thesis, we present a new immersed finite element (IFE) space for efficiently solving a class of interface problems on interface independent meshes. The new IFE space is formed by piecewise linear polynomials defined on sub-elements cut by the actual interface. We present the construction procedure for this IFE space and establish fundamental properties for its shape functions. Furthermore, we prove that the proposed IFE space has the optimal approximation capability.

Contents

List of Figures

List of Tables

Chapter 1

Introduction

In this chapter, we first provide a brief introduction to the typical second order elliptic interface problems and the related numerical methods in the literature in Section 1.1. In the second section, a survey of previous work about IFE methods will be given. In the last section, we describe the main contributions of this thesis to the study of IFE methods.

1.1 Interface Problems

Interface problems occur in many mathematical models in science and engineering. In such a model, a domain is partitioned by a curve or surface into subdomains in which materials have different physical or chemical properties. When a partial differential equation (PDE) is utilized in such a model, its coefficients are often discontinuous across the material interface. This leads to the so called interface problem for this PDE whose solution usually has a weaker regularity across the interface. The lack of regularity is a challenge for developing efficient numerical methods to solve interface problems.

In this thesis, we consider the typical second order elliptic boundary value problem:

$$-\nabla \cdot (\beta \nabla u) = f, \text{ in } \Omega, \tag{1.1}$$

$$u = g, \text{ on } \partial\Omega, \tag{1.2}$$

where the physical domain $\Omega \subset \mathbb{R}^2$ is formed by multiple materials. For simplicity and without loss of generality, we assume Ω is separated by an interface curve Γ into only two sub-domains Ω^+ and Ω^-, as shown in Figure 1.1. Because of the difference in material properties, the coefficient function $\beta(X)$ is discontinuous across the interface Γ. Here we shall assume $\beta(X)$ is a piecewise positive constant function defined by

$$\beta(X) = \begin{cases} \beta^-, & \text{if } X \in \Omega^-, \\ \beta^+, & \text{if } X \in \Omega^+. \end{cases}$$

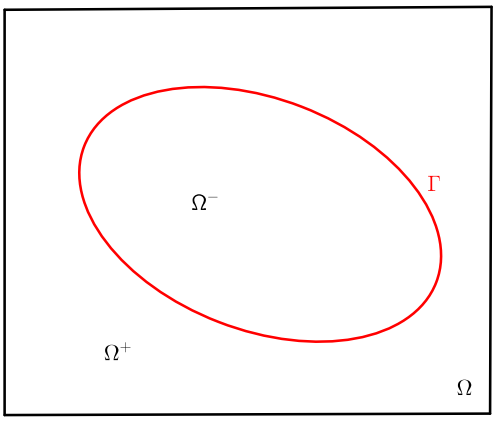

Figure 1.1: The physical domain of interface problems

The solution u is assumed to satisfy the following jump conditions:

$$[u]_\Gamma = 0, \tag{1.3a}$$
$$[\beta \nabla u \cdot \mathbf{n}]_\Gamma = 0, \tag{1.3b}$$

where $\mathbf{n}$ is the unit normal vector to the interface Γ, and for every piecewise function v such that

$$v = \begin{cases} v^-(X), & \text{if } X \in \Omega^-, \\ v^+(X), & \text{if } X \in \Omega^+, \end{cases}$$

we adopt the notation $[v]$ defined as $[v] = v^+|_\Gamma - v^-|_\Gamma$.

Due to the discontinuity of the coefficients β, the regularity of the exact solution u to the equation (1.1) and (1.3) is lower across the interface Γ which is a difficulty when solving interface problems. Generally speaking, two groups of numerical methods have been developed to solve interface problems. A finite element method in the traditional group has to use a body fitting mesh generated according to the interface Γ, [7, 11, 48]; otherwise, its performance cannot be guaranteed. This restriction prohibits an efficient application of finite element methods to mathematical models that involve moving interfaces. A representative example is the shape optimization problem [5, 16, 43] in which one seeks the optimal interface Γ^* such that

$$\Gamma^* = \text{argmin}_\Gamma \mathcal{J}(\Gamma; u(\Gamma)), \tag{1.4}$$

where $\mathcal{J}(\Gamma; u(\Gamma))$ is a functional depending on the interface Γ. Shape optimization problems in this formulation arise in many applications such as heat conduction problems [25, 41, 51] and Electrical Impedance Tomography (EIT) problems [12, 46]. In such applications, the location and geometry of the interface are driven to change by the optimization algorithm in each iteration. Generating meshes to fit a moving interface again and again in the optimiza-

tion iteration can be nontrivial and time consuming, especially when the interface geometry is complicated.

Recently, some efforts have been devoted to solving interface problems with interface independent meshes and this has yielded the second group of numerical methods for interface problems. For a problem with a moving interface, methods in the second group are advantageous than those in the traditional group because they do not need to remesh according to a moved interface. In an interface independent mesh, the interfaces must be allowed to cut the edges of elements, special techniques have to be developed to handle these elements intersecting with the interface. Generally speaking, two types of techniques have been developed that can generate optimally convergent schemes on interface independent meshes either in finite element or finite difference formulations. The first type of techniques modify a standard discretization formulation on interface elements. A typical example of such finite element schemes is the unfitted finite element methods using the Nitsche's penalty idea along the interface, see [4, 23] and references therein. For finite difference schemes, we refer readers to the immersed interface method (IIM) in [33, 35]. The second type of techniques focus on constructing local shape functions that can better capture the jump behaviors of interface problems, among which are the immersed finite element(IFE) methods in [17, 19, 21, 26, 32, 37, 40] and extended finite element methods(XFEM) in [4, 42]. These two types of techniques can also be employed together. For example, the authors in [24] developed an optimally convergent linear finite element method for interface problems that combines the Nitsche's penalty in the formulation and XFE spaces. Recently, the authors in [47] have extended this result to arbitrary p-th degree polynomials.

1.2 Previous works for IFE Methods

Since this thesis is to develop a new IFE space, we present a more detailed review in this section on previous works of IFE methods that motivate the research of this thesis. Since interface independent meshes are used for the IFE methods, the elements can be divided into interface elements and non-interface elements according to whether the interior of an element intersects the interface or not. IFE methods use the standard finite element shape functions on non-interface elements, but they utilize Hsieh-Clough-Tocher type macro finite element shape functions [6, 14] on interface elements. Each IFE shape function consists of two polynomials sitting on both sides of the interface, and these two polynomials are specially designed to handle the jump conditions across the interface in a certain sense.

The immersed finite element method was first introduced by Li in [34] to solve a 1-D elliptic interface problem using linear polynomials, and this idea was extended by Lin and Adjerid in [3] to arbitrary p-th degree polynomials. Recently the authors in [9] constructed IFE shape functions by orthogonal polynomials and studied their super-convergence properties for a 1-D elliptic interface problem. Due to the simple geometry, all the 1-D IFE shape functions presented in these publications can satisfy the jump conditions across the interface exactly.

However, for higher dimensional interface problems, we can no longer expect piecewise polynomials to exactly satisfy the jump conditions across general curve interfaces. In particular, two polynomials can not match exactly along a non-algebraic curve. Therefore, an IFE shape function has to be a piecewise polynomial whose components can satisfy the jump conditions only in an approximate sense. For IFE spaces based on lower degree polynomials, such as linear and bilinear polynomials, each IFE shape function on an interface element is constructed piecewisely on the two sub-elements cut by the line connecting the two points where the interface meets with the element edge, and the IFE shape function satisfies the jump condition on this line instead of the actual interface curve. But we note that this line is an $O(h^2)$ approximation to the interface curve inside the interface element and this $O(h^2)$ accuracy matches what we expect from the linear and bilinear polynomials. Within this framework, we refer readers to [17, 32, 36, 37] for linear IFE spaces, [32] for a linear Crouzeix-Raviart type IFE space, and [26, 27, 28] for bilinear IFE spaces. These spaces are all constructed by the standard Lagrangian type local degrees of freedom imposed either at the vertices of the elements or the midpoints of the element edges in an interface independent mesh.

Nevertheless, IFE methods are not standard finite element methods. Their shape functions in a macro polynomial form pose challenges for related error analysis. First, because of different interface locations in two interface elements, the pertinent functions spaces on two interface elements cannot be mapped to the same functions space on the reference elements through the standard affine mapping; hence, the powerful scaling argument in standard finite element error analysis cannot be applied to the error estimation for IFE spaces unless one can show that the scaling constant can be uniformly bounded for all interface elements. Instead, a generalized multipoint Taylor Expansion on interface elements has been employed to prove the optimal approximate capability of the linear IFE space in [36], the bilinear IFE in [26, 27, 28], and a rotated bilinear IFE space in [49]. Another issue is the discontinuity of IFE functions across interface edges. IFE shape functions in an interface element are constructed according to the interface configuration inside that interface element. Because of the different interface configurations in two adjacent interface elements, IFE shape functions in these two interface elements cannot match their values along the common interface edge between these adjacent interface elements except for those nodes where the degrees of freedom are imposed. As a consequence, the Lagrange type global IFE basis functions are continuous at all the nodes, but, in general, discontinuous across interface edges. This discontinuity is one of the obstacles for establishing the error bound for linear and bilinear IFE methods in [36, 27]. By adding penalty terms on interface edges into those IFE methods in [36, 27] to alleviate the impact of the edge discontinuity, the authors in [38] developed a group of partially penalized IFE methods whose optimal convergence has been proven. A rotated-Q_1 IFE space with the average integral value degrees of freedom on element edges was developed in [49] where the author also showed that the finite element method using this IFE space could converge optimally without using any penalty terms in the scheme.

There have been a few recent efforts to develop IFE spaces with higher order approxima-

tion capabilities. In [3], the authors introduced the idea of the extended jump conditions to construct optimally convergent p-th degree IFE spaces for a 1-D interface problem provided that the exact solution can satisfy the corresponding extended jump conditions. For interface problems in higher dimensions, two major obstacles exist in the development of the higher order IFE methods. The first one is how to partition an interface element into two subelements so that IFE shape functions in piecewise higher degree polynomial form can be constructed with the expected accuracy. Because of the intrinsic $\mathcal{O}(h^2)$ accuracy in the line approximating the interface curve, which is a fundamental feature of linear or bilinear IFE spaces, we would like to avoid constructing higher order IFE shape functions with subelements formed by a straight line. The second obstacle is how to enforce suitable extended jump conditions such that the IFE shape functions can be uniquely determined and the resulting IFE spaces can have optimal approximation capabilities.

To overcome the first obstacle, one natural idea is to construct IFE spaces formed by piecewise polynomials defined on sub-elements cut by the actual interface curve instead of its line approximation. By enforcing the jump conditions point-wisely on the actual interface, the authors in [21] derived an optimal error estimate which is independent of the ratio of β^- and β^+ for an IFE space constructed with linear polynomials. In [22], an optimal p-th order convergent IFE space for constant coefficients was investigated. In their construction, instead of imposing the actual normal vector, a constant normal vector is used to approximate the flux jump condition. Also, the authors in [18] developed a unified framework to construct IFE spaces defined by the curved subelements for linear, bilinear and rotated Q_1 polynomials, and the optimal approximation capability of these IFE spaces has been established by generalizing the multi-point Taylor expansion idea to discontinuous functions. A similar idea was used in [19] to construct and analyze a non-conforming IFE space using average integral value degrees of freedom and the curved subelements.

For the second obstacle, a linear interface and discontinuous coefficient case was discusses in [2] by imposing the following two different extended jump conditions,

$$\left[\beta\frac{\partial^j u}{\partial \mathbf{n}^j}\right]_\Gamma = 0, \quad j = 1, 2, \cdots, p, \tag{1.5}$$

$$\left[\beta\frac{\partial^j \triangle u}{\partial \mathbf{n}^j}\right]_\Gamma = 0, \quad j = 1.2 \cdots, p-1, \tag{1.6}$$

which are the higher order flux jump conditions and the higher order regularity of the right hand side f in (1.1). The authors in [1] generalized the idea above to curve interfaces by enforcing these extended jump conditions with the L^2 projection to pertinent polynomial spaces over the interface curve in the interface element. This means that the jump conditions are weakly enforced. However, the existence and uniqueness of the IFE shape functions in this framework are still elusive. In [45], a least squares method was developed to construct arbitrary p-th degree IFE spaces for both two types of the extended jump conditions given by (1.5) and (1.6). This method can always guaranty the existence of the IFE shape functions and the uniqueness can be proven under some specific conditions.

1.3 Contributions of this thesis

This thesis is based on the work of [18]. Its main efforts focus on the first obstacle mentioned above, i.e., the $\mathcal{O}(h^2)$ accuracy limitation of a line approximating a curve. For each interface element in a triangular mesh, we will develop a local IFE space formed by piecewise linear polynomials defined on sub-elements formed by partitioning the interface element by the actual interface curve instead of its line approximation. We hope the study of this IFE space defined by the actual interface can shed some light on the research of higher order IFE methods.

The IFE space constructed here are extended from those in [17, 32, 36, 27, 50] in the sense that the continuity condition is still imposed on the line connecting the intersection points of the interface with the element edges, but the flux jump condition is enforced on an arbitrary point on the interface. Together with the jump conditions, values at the vertices of elements are used as the degrees of freedom to determine the coefficients in an IFE shape function in the piecewise polynomial format in each interface element. By enforcing such weak jump conditions and nodal values, we show that the undetermined coefficients in an IFE shape function satisfy a Sherman-Morrison linear system. Furthermore, the invertibility of the Sherman-Morrison matrix guaranties the unisolvence of the IFE shape functions, i.e., the undetermined coefficients in an IFE shape function can be uniquely determined by the degrees of freedom imposed at the vertices of the interface element, and the invertibility is independent of how the interface cuts the elements. We note the IFE space in this thesis is similar to the one in [20], because in their construction of IFE space, the flux condition is still enforced at an arbitrary point on the interface and the continuity condition is enforced on the tangential line to the interface at the same point.

One of the challenges in estimating the interpolation errors of the IFE space developed in this thesis is the lower regularity. The IFE shape functions in each interface element are actually L^2 functions while the linear IFE shape functions in the literature such as [36, 27] are actually H^1 functions. Since it is still unclear how the elegant scaling argument can be applied to the error analysis of IFE methods, we will continue to utilize the idea of the multi-point Taylor expansion introduced in [36, 27] and generalize it to discontinuous functions. In particular, we will establish a group of fundamental identities showing how the two polynomial components in an IFE shape function are related to each other, and these identities are critical ingredients for us to derive error estimates for the IFE interpolation by using the generalized multi-point Taylor expansion. As a beneficial consequence of the fact that the partition of the IFE shape functions matches the actual partition of the interface elements by the interface curve, the error estimation for this new IFE space does not need to deal with the subdomain sandwiched between the line and the interface where special arguments had to be used to obtain error estimates for those IFE spaces in the literature [36, 27].

This thesis consists of three additional chapters organized as follows. In the next chapter,

some basic notations and fundamental assumptions about meshes and interfaces are given, which will be used throughout this thesis. Then we establish a group of geometric estimates and identities related to the interface. In the Chapter 2, we review and generalize the multi-point Taylor expansions for functions satisfying the jump conditions (1.3a) and (1.3b), and estimates for the remainders in these multi-point Taylor expansions are given. Towards to the end of Chapter 2, we will discuss quadrature rules on curved edge triangles and quadrilaterals, since the new IFE shape functions are all defined on curved edge sub-elements. In the Chapter 3, we first construct the IFE shape functions by using the weak jump conditions as well as nodal value conditions, which are used to form the local IFE spaces on interface elements. Then, a few basic properties of the IFE shape functions, including the boundedness, partition of unity and some fundamental identities are given. As the key result, we will prove the optimal convergence of the IFE interpolation by applying the multi-point Taylor expansion on the interpolation operators together with those fundamental properties established. Chapter 3 will end up by providing a group of numerical results. Finally Chapter 4 contains a brief summary and a brief future research plan.

Chapter 2

General IFE spaces

In this chapter, we first introduce some basic notations and assumptions. Then we consider general interface elements and study their geometric properties. Specifically, on interface elements, we show the estimates for the distance between the line connecting the intersection points and the interface curve as well as the difference between the normal vectors to the interface curve in terms of the mesh size h. Besides we construct a groups of matrices according to the jump conditions which are used to relate the exact solutions on two pieces. In the last section, we discuss the isoparametric mapping between curved edge triangles/quadrilaterals and reference triangles/quadrilaterals. This technique is used for the quadrature on curved edge sub-elements.

2.1 Preliminaries and Notations

Throughout the thesis, $\Omega \subset \mathbb{R}^2$ denotes a bounded domain formed by a union of triangular elements. Let $\mathcal{D}(\Omega)$ denote the space of $\mathcal{C}^\infty$ functions with compact supports in Ω. The dual space $\mathcal{D}'(\Omega)$ is the space of distributions. For any multi-index $\alpha = (\alpha_1, \alpha_2)$ with $|\alpha| = \alpha_1 + \alpha_2$, the weak derivative D^α of some function $v \in \mathcal{D}'(\Omega)$ is defined as

$$D^\alpha v(\phi) = (-1)^{|\alpha|} \int_\Omega (\frac{\partial^{|\alpha|}\phi}{\partial x^{\alpha_1} \partial y^{\alpha_2}}) v \, dxdy, \quad \forall \phi \in \mathcal{D}(\Omega).$$

And we use the following notations of Sobolev spaces:

$$W^{k,p}(\Omega) = \{v : \|v\|_{k,p,\Omega} < \infty\},$$

with the associated norm

$$\|v\|_{k,p,\Omega} = \left(\sum_{|\alpha| \leqslant k} \|D^\alpha v\|^p_{0,p,\Omega} \right)^{1/p},$$

where

$$\|v\|_{0,p,\Omega} = \left(\int_\Omega |v|^p dX \right)^{1/p},$$

for $1 \leqslant p < \infty$. If $p = \infty$, the norm is defined to be

$$\|v\|_{k,\infty,\Omega} = \max_{|\alpha| \leqslant k} \|D^\alpha v\|_{0,\infty,\Omega},$$

where

$$\|v\|_{0,\infty,\Omega} = \operatorname{ess\,sup}\{|v(X)| : X \in \Omega\}.$$

Also we define the Sobolev semi-norm as $|v|_{k,p,\Omega} = \|D^k v\|_{0,p,\Omega}$. And the special case is the Hilbert space, $H^k(\Omega) = W^{k,2}(\Omega)$. Since only the Hilbert space are used in this thesis, for simplicity we use $\|v\|_{k,\Omega} = \|v\|_{k,2,\Omega}$ and $|v|_{k,\Omega} = |v|_{k,2,\Omega}$.

Due to the discontinuity of first derivative from (1.3b), the solutions u to the interface problem have lower global regularity than the solutions to the usual elliptic PDEs, i.e $u \notin H^2(\Omega)$. However we note in each subdomain with some standard regularity assumptions on the interface and the source term f, $u|_{\Omega^s} \in H^2(\Omega^s)$, $s = +, -$, so it is convenient for us to use the following notations

$$PH^k(\Omega) = \{v : v|_{\Omega^s} \in H^k(\Omega^s),\ s = + \text{ or } -\}.$$

Moreover, according to the jump conditions (1.3a) and (1.3b), we define:

$$PH^k_{int}(\Omega) = \{u : u|_{\Omega^s} \in H^k(\Omega^s),\ s = + \text{ or } -;\ [u] = 0 \text{ and } [\beta \nabla u \cdot \mathbf{n}] = 0 \text{ on } \Gamma\},$$

$$PC^k_{int}(\Omega) = \{u : u|_{\Omega^s} \in C^k(\Omega^s),\ s = + \text{ or } -;\ [u] = 0 \text{ and } [\beta \nabla u \cdot \mathbf{n}] = 0 \text{ on } \Gamma\}.$$

And the associated norms and semi norms of $PH^k(\Omega)$ or $PH^k_{int}(\Omega)$ should be understood as

$$\|\cdot\|_{k,p,\Omega} = (\|\cdot\|^p_{k,p,\Omega^+} + \|\cdot\|^p_{k,p,\Omega^-})^{1/p},$$
$$|\cdot|_{k,p,\Omega} = (|\cdot|^p_{k,p,\Omega^+} + |\cdot|^p_{k,p,\Omega^-})^{1/p},$$

if $1 \leqslant p < \infty$, and

$$\|\cdot\|_{k,\infty,\Omega} = \max\{\|\cdot\|_{k,\infty,\Omega^+},\ \|\cdot\|_{k,\infty,\Omega^-}\},$$
$$|\cdot|_{k,p,\Omega} = \max\{|\cdot|_{k,\infty,\Omega^+}, |\cdot|_{k,\infty,\Omega^-}\},$$

if $p = \infty$.

Now let $\mathcal{T}_h$ be a mesh of the domain Ω with the size h. And $T \in \mathcal{T}_h$ is called an interface element if the interior of T intersects with the interface Γ; otherwise it is a non-interface element. Let $\mathcal{N}_h$ be the collection of all the nodes in the mesh. Besides, we will use the following notations:

- $\mathcal{T}_h^i$: the set of interface elements.
- $\mathcal{T}_h^n$: the set of non-interface elements.
- $\mathcal{E}_h^i$: the set of interface edges.
- $\mathcal{E}_h^n$: the set of non-interface edges.

For every interface element $T \in \mathcal{T}_h^i$, denote $T^+ = \Omega^+ \cap T$, $T^- = \Omega^- \cap T$. Similarly, we define

$$PH^k(T) = \{u : u|_{T^s} \in H^k(T^s),\ s = + \text{ or } -\},$$

$$PH^k_{int}(T) = \{u : u|_{T^s} \in H^k(T^s),\ s = + \text{ or } -;\ [u] = 0 \text{ and } [\beta \nabla u \cdot \mathbf{n}] = 0 \text{ on } \Gamma \cap T\},$$

$$PC^k_{int}(T) = \{u : u|_{T^s} \in C^k(T^s),\ s = + \text{ or } -;\ [u] = 0 \text{ and } [\beta \nabla u \cdot \mathbf{n}] = 0 \text{ on } \Gamma \cap T\},$$

with the norms and semi-norms

$$\|\cdot\|^2_{k,T} = \|\cdot\|^2_{k,T^+} + \|\cdot\|^2_{k,T^-}, \qquad |\cdot|^2_{k,T} = |\cdot|^2_{k,T^+} + |\cdot|^2_{k,T^-},$$

$$\|\cdot\|_{k,\infty,T} = \max\{\|\cdot\|_{k,\infty,T^+}\ ,\ \|\cdot\|_{k,\infty,T^-}\}, \qquad |\cdot|_{k,\infty,T} = \max\{|\cdot|_{k,\infty,T^+}\ ,\ |\cdot|_{k,\infty,T^-}\}.$$

In additional, as in [28], we assume that $\mathcal{T}_h$ satisfies the following hypotheses provided the mesh size h is small enough:

(H1) The interface Γ cannot intersect any edges with more than two points unless the edge is part of Γ.

(H2) If Γ intersects the boundary of an element at two points, these intersection points must be on different edges of this element.

(H3) The interface Γ is piecewise C^2 continuous, and the partition $\mathcal{T}_h$ is formed such that the subset of Γ in every interface element $T \in \mathcal{T}_h^i$ is C^2.

(H4) On each interface element $T \in \mathcal{T}_h^i$, $PC^2_{int}(T)$ is dense in $PH^2_{int}(T)$.

Finally, throughout this article, we let $\rho = \beta^-/\beta^+$. On any $T \in \mathcal{T}_h^i$, we use D, E to denote the intersection points of the interface curve with the element boundary and let l be the line connecting DE.

2.2 Geometric Properties of Interface Elements

All the analysis in this thesis is based on the geometric properties of interface elements in this section. For each interface element $T \in \mathcal{T}_h^i$, we consider a point $\widetilde{X}$ on $\Gamma \cap T$ and let $\mathbf{n}(X) = (\tilde{n}_x(\widetilde{X}), \tilde{n}_y(\widetilde{X}))$ be the unit normal vector to Γ at $\widetilde{X}$ from T^- to T^+. Also let $\widetilde{X}_\perp$ be the orthogonal projection of $\widetilde{X}$ onto l, where l is the straight line connecting the intersection points D and E. See Figure 2.1 for an illustration. We first estimate the difference between the normal vectors $\mathbf{n}(\widetilde{X})$ for various $\widetilde{X}$ and the distance between $\widetilde{X}$ and $\widetilde{X}_\perp$ in terms of the mesh size h.

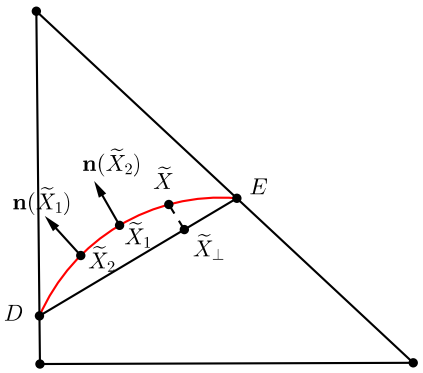

Figure 2.1: The geometry of an interface element

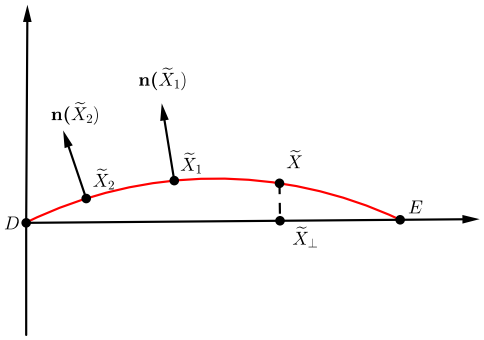

Figure 2.2: The local system

To show the estimation, we introduce a local coordinate system (ξ, η), with D being the origin point, l being the x-axis and the line through D orthogonal to l being the y-axis, as shown in Figure 2.2. Suppose in the local system, the function of the interface curve is $f(\xi)$. Recall the following lemma from [36]:

Lemma 2.1. *There exist constants C only depending on f, such that*

$$|f(\xi)| \leqslant Ch^2, \tag{2.1}$$

$$|f'(\xi)| \leqslant Ch. \tag{2.2}$$

Now we can use the Lemma 2.1 to show the following estimation.

Lemma 2.2. *There exist constants C independent of the interface location such that for any point $\widetilde{X} \in \Gamma \cap T$, the following inequalities hold:*

$$\|\widetilde{X} - \widetilde{X}_\perp\| \leqslant Ch^2, \tag{2.3}$$

and for any $\widetilde{X}_1,\ \widetilde{X}_2 \in \Gamma \cap T$*, there hold*

$$\|\mathbf{n}(\widetilde{X}_1) - \mathbf{n}(\widetilde{X}_2)\| \leqslant Ch, \tag{2.4a}$$

$$\mathbf{n}(\widetilde{X}_1) \cdot \mathbf{n}(\widetilde{X}_2) \geqslant 1 - Ch^2. \tag{2.4b}$$

Proof. (2.3) is directly from (2.1) in the Lemma 2.1. For (2.4a), we can suppose in the local system, $\widetilde{X}_1$ and $\widetilde{X}_2$ have the coordinates $(\xi_1, f(\xi_2))$ and $(\xi_2, f(\xi_2))$ respectively. Then we have

$$\mathbf{n}(\widetilde{X}_1) = \frac{1}{\sqrt{1+(f'(\xi_1))^2}} \begin{pmatrix} -f'(\xi_1) \\ 1 \end{pmatrix}, \quad \mathbf{n}(\widetilde{X}_2) = \frac{1}{\sqrt{1+(f'(\xi_2))^2}} \begin{pmatrix} -f'(\xi_2) \\ 1 \end{pmatrix}.$$

Note that (2.2) yields

$$\left| \frac{f'(\xi_1)}{\sqrt{1+(f'(\xi_1))^2}} - \frac{f'(\xi_2)}{\sqrt{1+(f'(\xi_2))^2}} \right| \leqslant \left| \frac{f'(\xi_1)}{\sqrt{1+(f'(\xi_1))^2}} \right| + \left| \frac{f'(\xi_2)}{\sqrt{1+(f'(\xi_2))^2}} \right| \leqslant Ch,$$

and

$$\begin{aligned}
&\left| \frac{1}{\sqrt{1+(f'(\xi_1))^2}} - \frac{1}{\sqrt{1+(f'(\xi_2))^2}} \right| \\
=&\left| \frac{\sqrt{1+(f'(\xi_2))^2} - \sqrt{1+(f'(\xi_1))^2}}{\sqrt{1+(f'(\xi_2))^2}\sqrt{1+(f'(\xi_1))^2}} \right| \\
\leqslant&\left| \sqrt{1+(f'(\xi_2))^2} - \sqrt{1+(f'(\xi_1))^2} \right| \\
=&\frac{|(f'(\xi_2))^2 - (f'(\xi_1))^2|}{\sqrt{1+(f'(\xi_2))^2} + \sqrt{1+(f'(\xi_1))^2}} \\
\leqslant&Ch^2.
\end{aligned}$$

Combining the inequalities, we have (2.4a). Besides it is easy to see that

$$C^2h^2 \geqslant \|\mathbf{n}(\widetilde{X}_1) - \mathbf{n}(\widetilde{X}_2)\|^2 = \|\mathbf{n}(\widetilde{X}_1)\|^2 + \|\mathbf{n}(\widetilde{X}_2)\|^2 - 2\mathbf{n}(\widetilde{X}_1) \cdot \mathbf{n}(\widetilde{X}_2) = 2 - 2\mathbf{n}(\widetilde{X}_1) \cdot \mathbf{n}(\widetilde{X}_2).$$

which yields (2.4b). □

Remark 2.1. *From the Cauchy's theorem, there is some point* $(\xi_0, f(\xi_0))$ *such that* $f'(\xi_0) = 0$ *which means the normal vector at this point is identical to the normal vector to the line* l*,* $\bar{\mathbf{n}}$*. So specifically, we can take* $\widetilde{X}_1$ *to be the point corresponding to local coordinates* $(\xi_0, f(\xi_0))$ *in Lemma 2.2. Hence for any* $\widetilde{X} \in \Gamma \cap T$*, we have*

$$\|\mathbf{n}(\widetilde{X}) - \bar{\mathbf{n}}\| \leqslant Ch, \tag{2.5a}$$

$$\mathbf{n}(\widetilde{X}) \cdot \bar{\mathbf{n}} \geqslant 1 - Ch^2. \tag{2.5b}$$

The estimates above indicate that the normal vectors to the curve and to the line would be very close to each other when the element is small enough.

Now using both the continuity conditions and the flux jump conditions, we construct a group of matrices to describe the relation between the gradients of the true solutions sitting on the two sides of the interface. For any $\widetilde{X} \in \Gamma \cap T$, we define $\mathbf{n}(\widetilde{X}) = (\tilde{n}_x, \tilde{n}_y)$ for convenience of presentation. Consider the following two matrices

$$N^-(\widetilde{X}) = \begin{pmatrix} \tilde{n}_y & -\tilde{n}_x \\ \beta^- \tilde{n}_x & \beta^- \tilde{n}_y \end{pmatrix} \quad \text{and} \quad N^+(\widetilde{X}) = \begin{pmatrix} \tilde{n}_y & -\tilde{n}_x \\ \beta^+ \tilde{n}_x & \beta^+ \tilde{n}_y \end{pmatrix}.$$

Note that $Det(N^-(\widetilde{Y})) = \beta^-$ and $Det(N^+(\widetilde{Y})) = \beta^+$. Then we can define

$$M^-(\widetilde{X}) = \left(N^+(\widetilde{X})\right)^{-1} N^-(\widetilde{X}) = \begin{pmatrix} \tilde{n}_y^2 + \rho \tilde{n}_x^2 & (\rho - 1)\tilde{n}_x \tilde{n}_y \\ (\rho - 1)\tilde{n}_x \tilde{n}_y & \tilde{n}_x^2 + \rho \tilde{n}_y^2 \end{pmatrix}, \tag{2.6}$$

$$M^+(\widetilde{X}) = \left(N^-(\widetilde{X})\right)^{-1} N^+(\widetilde{X}) = \begin{pmatrix} \tilde{n}_y^2 + 1/\rho \tilde{n}_x^2 & (1/\rho - 1)\tilde{n}_x \tilde{n}_y \\ (1/\rho - 1)\tilde{n}_x \tilde{n}_y & \tilde{n}_x^2 + 1/\rho \tilde{n}_y^2 \end{pmatrix}. \tag{2.7}$$

The matrices above are used to relate the gradients of u on the two pieces. Indeed for every $u \in PC^2_{int}(T)$, we have

$$\nabla u^+(\widetilde{X}) = M^-(\widetilde{X}) \nabla u^-(\widetilde{X}), \qquad \nabla u^-(\widetilde{X}) = M^+(\widetilde{X}) \nabla u^+(\widetilde{X}). \tag{2.8}$$

We further define the following two matrices:

$$\overline{N}^-(\widetilde{X}) = \begin{pmatrix} \bar{n}_y & -\bar{n}_x \\ \beta^- \tilde{n}_x & \beta^- \tilde{n}_y \end{pmatrix} \quad \text{and} \quad \overline{N}^+(\widetilde{X}) = \begin{pmatrix} \bar{n}_y & -\bar{n}_x \\ \beta^+ \tilde{n}_x & \beta^+ \tilde{n}_y \end{pmatrix}.$$

Note that Lemma 2.2 implies

$$Det(\overline{N}^{\pm}(\widetilde{X})) = \beta^{\pm}(\bar{n}_x \tilde{n}_x + \bar{n}_y \tilde{n}_y) = \beta^{\pm} \mathbf{n}(\widetilde{X}) \cdot \bar{\mathbf{n}} \geqslant \beta^{\pm}(1 - Ch^2),$$

which means $\overline{N}^{\pm}$ are non-singular if h is small enough. Similar to (2.6) and (2.7), we consider

$$\overline{M}^+(\widetilde{X}) = (\overline{N}^-(\widetilde{X}))^{-1} \overline{N}^+(\widetilde{X}), \quad \overline{M}^- = (\overline{N}^+(\widetilde{X}))^{-1} \overline{N}^-(\widetilde{X}). \tag{2.9}$$

And by direct calculations, we have

$$\overline{M}^+(\widetilde{X}) = \frac{1}{\bar{n}_x \tilde{n}_x + \bar{n}_y \tilde{n}_y} \begin{pmatrix} \bar{n}_y \tilde{n}_y + \frac{1}{\rho} \bar{n}_x \tilde{n}_x & -\tilde{n}_y \bar{n}_x + \frac{1}{\rho} \bar{n}_x \tilde{n}_y \\ -\tilde{n}_x \bar{n}_y + \frac{1}{\rho} \bar{n}_y \tilde{n}_x & \bar{n}_x \tilde{n}_x + \frac{1}{\rho} \bar{n}_y \tilde{n}_y \end{pmatrix}, \tag{2.10a}$$

$$\overline{M}^-(\widetilde{X}) = \frac{1}{\bar{n}_x \tilde{n}_x + \bar{n}_y \tilde{n}_y} \begin{pmatrix} \bar{n}_y \tilde{n}_y + \rho \bar{n}_x \tilde{n}_x & -\tilde{n}_y \bar{n}_x + \rho \bar{n}_x \tilde{n}_y \\ -\tilde{n}_x \bar{n}_y + \rho \bar{n}_y \tilde{n}_x & \bar{n}_x \tilde{n}_x + \rho \bar{n}_y \tilde{n}_y \end{pmatrix}. \tag{2.10b}$$

The following results show that matrices $\overline{M}^{\pm}$ are the approximation to matrices $M^{\pm}$.

Lemma 2.3. *For any interface element with mesh size h small enough, there exists a constant C independent of interface location, such that, for arbitrary two points $\widetilde{X}_i, i = 1, 2$ on $\Gamma \cap T$, the following inequality holds*

$$\|\overline{M}^s(\widetilde{X}_1) - M^s(\widetilde{X}_2)\| \leqslant Ch, \quad s = \pm. \tag{2.11}$$

Proof. We only show the case $s = -$ and the argument for $s = +$ is similar. By the triangular inequality, we have

$$\begin{aligned} &\|\overline{M}^-(\widetilde{X}_1) - M^-(\widetilde{X}_2)\| = \|(\overline{N}^+(\widetilde{X}_1))^{-1}\overline{N}^-(\widetilde{X}_1) - (N^+(\widetilde{X}_2))^{-1}N^-(\widetilde{X}_2)\| \\ &\leq \|(\overline{N}^+(\widetilde{X}_1))^{-1}\|\,\|\overline{N}^-(\widetilde{X}_1) - N^-(\widetilde{X}_2)\| + \|(\overline{N}^+(\widetilde{X}_1))^{-1} - (N^+(\widetilde{X}_2))^{-1}\|\,\|N^-(\widetilde{X}_2)\|. \end{aligned} \tag{2.12}$$

The Lemma 2.2 and Remark 2.1 imply

$$\|\overline{N}^-(\widetilde{X}_1) - N^-(\widetilde{X}_2)\| = \left\| \begin{pmatrix} \bar{n}_y - \tilde{n}_y(\widetilde{X}_2) & -\bar{n}_x + \tilde{n}_x(\widetilde{X}_2) \\ \beta^-(\tilde{n}_x(\widetilde{X}_1) - \tilde{n}_x(\widetilde{X}_2)) & \beta^-(\tilde{n}_y(\widetilde{X}_1) - \tilde{n}_y(\widetilde{X}_2)) \end{pmatrix} \right\| \leqslant Ch. \tag{2.13}$$

Besides, we note the following identity

$$\begin{aligned} &(\overline{N}^+(\widetilde{X}_1))^{-1} - (N^+(\widetilde{X}_2))^{-1} \\ =&\frac{1}{\beta^+\mathbf{n}(\widetilde{X}_1)\cdot\bar{\mathbf{n}}} \begin{pmatrix} \beta^+\tilde{n}_y(\widetilde{X}_1) & \bar{n}_x \\ -\beta^+\tilde{n}_x(\widetilde{X}_1) & \bar{n}_y \end{pmatrix} - \frac{1}{\beta^+} \begin{pmatrix} \beta^+\tilde{n}_y(\widetilde{X}_2) & \tilde{n}_x(\widetilde{X}_2) \\ -\beta^+\tilde{n}_x(\widetilde{X}_2) & \tilde{n}_y(\widetilde{X}_2) \end{pmatrix} \\ =&\frac{1}{\beta^+\mathbf{n}(\widetilde{X}_1)\cdot\bar{\mathbf{n}}} \begin{pmatrix} \beta^+(\tilde{n}_y(\widetilde{X}_1) - \tilde{n}_y(\widetilde{X}_2)) & (\bar{n}_x - \tilde{n}_x(\widetilde{X}_2)) \\ -\beta^+(\tilde{n}_x(\widetilde{X}_1) - \tilde{n}_x(\widetilde{X}_2)) & (\bar{n}_y - \tilde{n}_y(\widetilde{X}_2)) \end{pmatrix} \\ &+ \frac{1 - \mathbf{n}(\widetilde{X}_1)\cdot\bar{\mathbf{n}}}{\beta^+\mathbf{n}(\widetilde{X}_1)\cdot\bar{\mathbf{n}}} \begin{pmatrix} \beta^+\tilde{n}_y(\widetilde{X}_2) & \tilde{n}_x(\widetilde{X}_2) \\ -\beta^+\tilde{n}_x(\widetilde{X}_2) & \tilde{n}_y(\widetilde{X}_2) \end{pmatrix}. \end{aligned}$$

Then, combining Lemma 2.2 and the identity above yields

$$\left\|(\overline{N}^+(\widetilde{X}_1))^{-1} - (N^+(\widetilde{X}_2))^{-1}\right\| \leqslant Ch. \tag{2.14}$$

Finally, applying estimates (2.13) and (2.14) to (2.12) leads to the inequality (2.11). □

Taking $\bar{\mathbf{t}} = (\bar{n}_y, -\bar{n}_x)^T$ to be the tangential vector of l, it is important to note that $\overline{M}^\pm$ has the following properties:

Lemma 2.4. *$\overline{M}^+(\widetilde{X})$ and $\overline{M}^-(\widetilde{X})$ are inverse matrices to each other. $(\overline{M}^+(\widetilde{X}))^T$ has two eigenvalues 1 and $1/\rho$ with the corresponding eigenvectors $\bar{\mathbf{t}}$ and $\mathbf{n}(\widetilde{X})$, respectively. And similarly, $(\overline{M}^-(\widetilde{X}))^T$ has two eigenvalues 1 and ρ with the corresponding eigenvectors $\bar{\mathbf{t}}$ and $\mathbf{n}(\widetilde{X})$, respectively. In another word, we have*

$$\overline{M}^-(\widetilde{X})\overline{M}^+(\widetilde{X}) = I, \tag{2.15}$$

$$\left(\overline{M}^{-}(\widetilde{X})\right)^{T}\bar{\mathbf{t}}=\bar{\mathbf{t}},\quad \left(\overline{M}^{+}(\widetilde{X})\right)^{T}\bar{\mathbf{t}}=\bar{\mathbf{t}}, \tag{2.16}$$

$$\left(\overline{M}^{-}(\widetilde{X})\right)^{T}\mathbf{n}(\widetilde{X})=\rho\mathbf{n}(\widetilde{X}),\quad \left(\overline{M}^{+}(\widetilde{X})\right)^{T}\mathbf{n}(\widetilde{X})=\frac{1}{\rho}\mathbf{n}(\widetilde{X}). \tag{2.17}$$

Proof. . First it is easy to see that $\overline{M}^{-}(\widetilde{X})\overline{M}^{+}(\widetilde{X})=(\overline{N}^{-}(\widetilde{X}))^{-1}\overline{N}^{+}(\widetilde{X})(\overline{N}^{+}(\widetilde{X}))^{-1}\overline{N}^{-}(\widetilde{X})=I$. Next by direct calculation, we have

$$\begin{aligned}(\overline{M}^{-}(\widetilde{X}))^{T}\bar{\mathbf{t}}&=\frac{1}{\bar{n}_x\tilde{n}_x+\bar{n}_y\tilde{n}_y}\begin{pmatrix}\bar{n}_y\tilde{n}_y+\rho\bar{n}_x\tilde{n}_x & -\tilde{n}_x\bar{n}_y+\rho\bar{n}_y\tilde{n}_x\\ -\tilde{n}_y\bar{n}_x+\rho\bar{n}_x\tilde{n}_y & \bar{n}_x\tilde{n}_x+\rho\bar{n}_y\tilde{n}_y\end{pmatrix}\begin{pmatrix}\bar{n}_y\\ -\bar{n}_x\end{pmatrix}\\ &=\frac{1}{\bar{n}_x\tilde{n}_x+\bar{n}_y\tilde{n}_y}\begin{pmatrix}\bar{n}_y(\bar{n}_x\tilde{n}_x+\bar{n}_y\tilde{n}_y)\\ -\bar{n}_x(\bar{n}_x\tilde{n}_x+\bar{n}_y\tilde{n}_y)\end{pmatrix}\\ &=\begin{pmatrix}\bar{n}_y\\ -\bar{n}_x\end{pmatrix},\end{aligned}$$

which is exactly $\bar{\mathbf{t}}$. By similar calculation, we can easily check that $(\overline{M}^{-}(\widetilde{X}))^{T}\mathbf{n}(\widetilde{X})=\rho\,\mathbf{n}(\widetilde{X})$. The results about $(\overline{M}^{+}(\widetilde{X}))^{T}$ follow from the fact $(\overline{M}^{-}(\widetilde{X}))^{T}(\overline{M}^{+}(\widetilde{X}))^{T}=I$. □

The following lemma is a simple but important corollary of Lemma 2.4.

Lemma 2.5. *Given any fixed point P, then the following two vectors*

$$(\overline{M}^{+}(\widetilde{X})-I)^{T}(P-\overline{X})\quad \textit{and}\quad (\overline{M}^{-}(\widetilde{X})-I)^{T}(P-\overline{X})$$

are both constant vectors for any arbitrary $\overline{X}$ moving along l.

Proof. Suppose $\overline{X}$ and $\overline{X}'$ are two arbitrary points on l. Note that $\overline{X}'-\overline{X}$ has the same direction as $\bar{\mathbf{t}}$. So (2.16) indicates that

$$\begin{aligned}&(\overline{M}^{+}(\widetilde{X})-I)^{T}(P-\overline{X})-(\overline{M}^{+}(\widetilde{X})-I)^{T}(P-\overline{X}')\\ =&(\overline{M}^{+}(\widetilde{X})-I)^{T}(\overline{X}'-\overline{X})\\ =&\|\overline{X}'-\overline{X}\|(\overline{M}^{+}-I)^{T}\bar{\mathbf{t}}\\ =&0\end{aligned}$$

which finishes the proof. □

2.3 Multipoint Taylor Expansion

In this section, we first review the multipoint Taylor expansion of $u \in PC^2_{int}(T)$ on every interface element T, i.e., we expand $u(X)$, $X \in T$, around the $T's$ vertices A_i, $i = 1, 2, 3$. Then we present the estimates for the remainders in the expansions, which are based on [8, 10]. In the following discussion, without loss of generality, we assume the interface T has the configuration illustrated in Figure 2.3, and we only consider the case $X \in T^+$, the argument for $X \in T^-$ is similar. Let $\mathcal{I}$ be the index set of vertices of T, i.e., $\mathcal{I} = \{1, 2, 3\}$. Suppose $\mathcal{I}$ is partitioned by the interface to two sets: $\mathcal{I}^+ = \{A_i : A_i \in T^+, i \in \mathcal{I}\}$ and $\mathcal{I}^- = \{A_i : A_i \in T^-, i \in \mathcal{I}\}$.

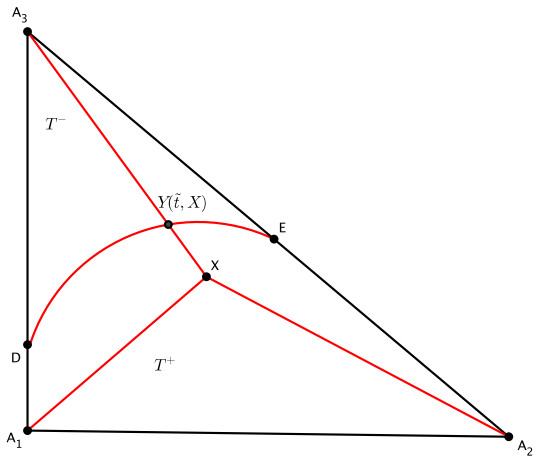

Figure 2.3: The expansion of u on triangular elements. (P is one of A_i.)

Given any $X \in T^+$, define $Y_i(t, X) = tA_i + (1 - t)X$. Denote

$$R_i(X) = \int_0^1 (1 - t)\frac{d^2}{dt^2}u^+(Y_i(t, X))dt, \quad i \in \mathcal{I}^+. \tag{2.18}$$

Then the standard second order Taylor expansion of $u \in PC^2_{int}(T)$ is

$$u^+(A_i) = u^+(X) + \nabla u^+(X) \cdot (A_i - X) + R_i(X), \quad i \in \mathcal{I}^+. \tag{2.19}$$

However, if $i \in \mathcal{I}^-$, due to the jump conditions along the curve, the expansion of $u^-(A_i)$ is not as simple as (2.19). Note that there exists $\tilde{t}_i \in [0, 1]$ such that $\widetilde{Y}_i = Y_i(\tilde{t}, X)$ is on the curve $\Gamma \cap T$. Then the expansion is given by the following lemma according to [27, 36, 49].

Lemma 2.6. *Assume $i \in \mathcal{I}^-$, $X \in T^+$ and $u \in PC^2_{int}(T)$. Denote*

$$R_i(X) = R_{i1} + R_{i2} + R_{i3}, \tag{2.20}$$

where

$$R_{i1}(X) = \int_0^{\tilde{t}_i} (1-t)\frac{d^2u^+}{dt^2}(Y_i(t,X))dt, \tag{2.21a}$$

$$R_{i2}(X) = \int_{\tilde{t}_i}^1 (1-t)\frac{d^2u^-}{dt^2}(Y_i(t,X))dt, \tag{2.21b}$$

$$R_{i3}(X) = (1-\tilde{t}_i)\int_0^{\tilde{t}_i} \frac{d}{dt}\left((M^+(\widetilde{Y}_i) - I)\nabla u^-(Y_i(t,X))\cdot(A_i - X)\right)dt, \tag{2.21c}$$

and $M^+(\widetilde{Y}_i)$ *is from* (2.7). *Then the expansion of* u *is given by*

$$\begin{aligned} u^-(A_i) =& u^+(X) + \nabla u^+(X)\cdot(A_i - X) \\ &+ \left(\left(M^+(\widetilde{Y}_i) - I\right)\nabla u^+(X)\right)\cdot(A_i - \widetilde{Y}_i) + R_i(X). \end{aligned} \tag{2.22}$$

Proof. First, from the continuity of u along the curve, we have

$$u^-(A_i) = u^+(X) + \int_0^{\tilde{t}_i} \frac{du^+}{dt}(Y_i(t,X))dt + \int_{\tilde{t}_i}^1 \frac{du^-}{dt}(Y_i(t,X))dt. \tag{2.23}$$

Note that

$$\begin{aligned} &\int_0^{\tilde{t}_i} \frac{du^+}{dt}(Y_i(t,X))dt \\ =& -\int_0^{\tilde{t}_i} \frac{du^+}{dt}(Y_i(t,X))d(1-t) \\ =& -\left[(1-t)\frac{du^+}{dt}(Y_i(t,X))|_0^{\tilde{t}_i} - \int_0^{\tilde{t}_i}(1-t)\frac{d^2u^+}{dt^2}(Y_i(t,X))dt\right] \\ =& -\left[(1-t)\nabla u^+(Y_i(t,X))\cdot\frac{dY_i(t,x)}{dt}|_0^{\tilde{t}_i} - \int_0^{\tilde{t}_i}(1-t)\frac{d^2u^+}{dt^2}(Y_i(t,X))dt\right] \\ =& -\left[(1-t)\nabla u^+(Y_i(t,X))\cdot(A_i - X)|_0^{\tilde{t}_i} - \int_0^{\tilde{t}_i}(1-t)\frac{d^2u^+}{dt^2}(Y_i(t,X))dt\right] \\ =& -\nabla u^+(\widetilde{Y}_i)\cdot(A_i - \widetilde{Y}_i) + \nabla u^+(X)\cdot(A_i - X) \\ &+ \int_0^{\tilde{t}_i}(1-t)\frac{d^2u^+}{dt^2}(Y_i(t,X))dt, \end{aligned} \tag{2.24}$$

where we use the identity $A_i - Y_i(t,X) = (1-t)(A_i - X)$. And similarly, we have

$$\begin{aligned}
&\int_{\tilde{t}_i}^1 \frac{du^-}{dt}(Y_i(t,X))dt \\
=&-\int_{\tilde{t}_i}^1 \frac{du^-}{dt}(Y_i(t,X))d(1-t) \\
=&-\left[(1-t)\frac{du^-}{dt}(Y_i(t,X))|_{\tilde{t}_i}^1 - \int_{\tilde{t}_i}^1 (1-t)\frac{d^2u^-}{dt^2}(Y_i(t,X))dt\right] \\
=&\nabla u^-(\widetilde{Y}_i)\cdot(A_i - \widetilde{Y}_i) + \int_{\tilde{t}_i}^1 (1-t)\frac{d^2u^-}{dt^2}(Y_i(t,X))dt.
\end{aligned} \tag{2.25}$$

So substituting (2.24) and (2.25) into (2.23) yields

$$\begin{aligned}
u^-(A_i) = &\, u^+(X) + \nabla u^+(X)\cdot(A_i - X) \\
&+ \left(\nabla u^-(\widetilde{Y}_i) - \nabla u^+(\widetilde{Y}_i)\right)\cdot(A_i - \widetilde{Y}_i) \\
&+ \int_0^{\tilde{t}_i}(1-t)\frac{d^2u^+}{dt^2}(Y_i(t,X))dt + \int_{\tilde{t}_i}^1 (1-t)\frac{d^2u^+}{dt^2}(Y_i(t,X))dt.
\end{aligned} \tag{2.26}$$

Finally, note that

$$\begin{aligned}
&\left(\nabla u^-(\widetilde{Y}_i) - \nabla u^+(\widetilde{Y}_i)\right)\cdot(A_i - \widetilde{Y}_i) \\
=&\left(M^+(\widetilde{Y}_i) - I\right)\nabla u^+(\widetilde{Y}_i)\cdot(A_i - \widetilde{Y}_i) \\
=&(1-\tilde{t}_i)\int_0^{\tilde{t}_i}\frac{d}{dt}\left((M^+(\widetilde{Y}_i) - I)\nabla u^+(Y_i(t,X))\cdot(A_i - X)\right)dt \\
&+\left(M^+(\widetilde{Y}_i) - I\right)\nabla u^+(X)\cdot(A_i - \widetilde{Y}_i),
\end{aligned} \tag{2.27}$$

which yields the desired identity (2.22). □

Now we show the estimation of the second order terms given by (2.19) and (2.22).

Lemma 2.7. *Suppose $u \in PC^2_{int}(T)$. Then there exits a constant $C > 0$ independent of the interface location such that*

$$\int_{T^+}(1-t)^2|u_{sr}(Y_i(t,X))|^2dX \leqslant C|u|^2_{2,T}, \qquad s = +,-, \quad i \in \mathcal{I}, \tag{2.28}$$

where s=x or y and r =x or y.

Proof. Let $A_i = (x_i, y_i)$ and consider the variable change $\xi = tx_i + (1-t)x$ and $\eta = ty_i + (1-t)y$ for fixed $t \in [0,1]$. Under this variable change, the new domain is

$$T^+(t) = \{tA_i + (1-t)X | X \in T^+\}.$$

Since $A_i \in T^+$, $T^+(t)$ must be the subset of T^+ for fixed t. However if $A_i \in T^-$, it may not be true, since $\tilde{t}_i = \tilde{t}_i(X)$ depends on X. But $T^+(t)$ must be the subset of T. So we need to estimate the integral on the whole element T. Actually it is not hard to see that

$$\begin{aligned}
&\int_{T^+} (1-t)^2 |u_{sr}(Y(t,X))|^2 dX \\
=&\int_{T^+} (1-t)^2 |u_{sr}(tx_P + (1-t)x, ty_P + (1-t)y)|^2 dxdy \\
=&\int_{T^+(t)} (1-t)^2 u_{sr}^2(\xi,\eta)(1-t)^{-2} d\xi d\eta \leqslant |u|_{2,T}^2,
\end{aligned}$$

which leads to (2.28). □

Now for the remainders in (2.19) nad (2.22), one can easily verify that

$$\begin{aligned}
\frac{d^2}{dt^2} u(Y_i(t,X)) =& u_{xx}(Y_i(t,X))(x_i - x)^2 + u_{xy}(Y_i(t,X))(x_i - x)(y_i - y) \\
& u_{yx}(Y_i(t,X))(x_i - x)(y_i - y) + u_{yy}(Y_i(t,X))(y_i - y)^2 \\
=& (A_i - X)^T H_u(Y_i(t,X))(A_i - X),
\end{aligned}$$

where

$$H_u(Y_i(t,X)) = \begin{pmatrix} u_{xx}(Y_i(t,x)) & u_{xy}(Y_i(t,x)) \\ u_{yx}(Y_i(t,x)) & u_{yy}(Y_i(t,x)) \end{pmatrix}$$

is the Hessian matrix of u. Then we have

Lemma 2.8. *Assume $u \in PC_{int}^2(T)$, then there exist constants $C > 0$ independent of the location of the interface such that*

$$\|R_i\|_{0,T^+} \leqslant Ch^2 |u|_{2,T}, \qquad i \in \mathcal{I}^+. \tag{2.29}$$

Proof. According to Lemma 2.7, we have

$$\begin{aligned}
\|R_i\|_{0,T^+} =& \left(\int_{T^+} \left(\int_0^1 (1-t)(A_i - X) H_u(Y_i(t,X))(A_i - X) dt \right)^2 dX \right)^{\frac{1}{2}} \\
\leqslant& Ch^2 \left(\int_{T^+} \left(\int_0^1 (1-t)(|u_{xx}(Y_i(t,X))| + |u_{xy}(Y_i(t,X))| + |u_{yy}(Y_i(t,X))|) dt \right)^2 dX \right)^{\frac{1}{2}} \\
\leqslant& Ch^2 \int_0^1 \left(\int_{T^+} (1-t)^2 (|u_{xx}(Y_i(t,X))| + |u_{xy}(Y_i(t,X))| + |u_{yy}(Y_i(t,X))|)^2 dX \right)^{\frac{1}{2}} dt \\
\leqslant& Ch^2 \int_0^1 \left(\int_{T^+} (1-t)^2 (|u_{xx}(Y_i(t,X))|^2 + |u_{xy}(Y_i(t,X))|^2 + |u_{yy}(Y_i(t,X))|^2) dX \right)^{\frac{1}{2}} dt \\
\leqslant& Ch^2 |u|_{2,T}^2,
\end{aligned}$$

where the second inequality is due to the Minkovski inequality. □

Lemma 2.9. *Assume $u \in PC^2_{int}(T)$, then there exist constants $C > 0$ independent of the interface location such that*

$$\|R_{i1}\|_{0,T^+} \leqslant Ch^2|u|_{2,T}, \tag{2.30a}$$
$$\|R_{i2}\|_{0,T^+} \leqslant Ch^2|u|_{2,T}. \tag{2.30b}$$

Proof. Note that in (2.21a) and (2.21b), $\tilde{t}_i$ is between 0 and 1. So the proof is same as Lemma 2.8. □

Now, to estimate R_{i3}, we first note that

$$\begin{aligned}
&\frac{d}{dt}\left((M^+(\widetilde{Y}_i) - I)\nabla u^-(Y_i(t,X)) \cdot (A_i - X)\right) \\
=&(\frac{d}{dt}\nabla u^-(Y_i(t,X)))^T(M^+(\widetilde{Y}_i) - I)^T(A_i - X) \\
=&(A_i - X)^T H_u(Y_i(t,X))(M^+(\widetilde{Y}_i) - I)^T(A_i - X).
\end{aligned} \tag{2.31}$$

Hence we finally have

Lemma 2.10. *Assume $u \in PC^2_{int}(T)$, then there exist constants $C > 0$ independent of the interface location such that*

$$\|R_{i3}\|_{0,T^+} \leqslant Ch^2|u|_{2,T}. \tag{2.32}$$

Proof. Note that $0 \leqslant 1 - \tilde{t}_i(X) \leqslant 1 - t$ for any $t \in [0, \tilde{t}_i(X)]$, then (2.31) leads to

$$\begin{aligned}
\|R_{i3}\|_{0,T^+} =& \left(\int_{T^+}(1-\tilde{t}_i(X))^2\left(\int_0^{\tilde{t}_i(X)}(A_i - X)^T H_u(Y_i(t,X))(M^+(\widetilde{Y}_i) - I)^T(A_i - X)dt\right)^2 dX\right)^{\frac{1}{2}} \\
=& \left(\int_{T^+}\left(\int_0^{\tilde{t}_i(X)}(1-\tilde{t}_i(X))\ (A_i - X)^T H_u(Y_i(t,X))(M^+(\widetilde{Y}_i) - I)^T(A_i - X)dt\right)^2 dX\right)^{\frac{1}{2}} \\
\leqslant& Ch^2\left(\int_{T^+}\left(\int_0^1 |1-t|\ \left(|u_{xx}(Y_i(t,X))| + |u_{xy}(Y_i(t,X))| + |u_{yy}(Y_i(t,X))|\right)dt\right)^2 dX\right)^{\frac{1}{2}} \\
\leqslant& Ch^2\int_0^1\left(\int_{T^+}(1-t)^2(|u_{xx}(Y_i(t,X))|^2 + |u_{xy}(Y_i(t,X))|^2 + |u_{yy}(Y_i(t,X))|^2)dX\right)^{\frac{1}{2}}dt \\
\leqslant& Ch^2|u|^2_{2,T},
\end{aligned}$$

where we use the Minkovski inequality and Lemma 2.7. □

2.4 Quadrature On Curved-Sided Domain

In this thesis, our IFE space will be constructed by partitioning the elements with the interface curve. So the technique of numerical integration on a domain with a curved boundary is critical in computation. In this section, we describe quadrature rules on curve-sided triangles and quadrilateral. The idea is based on *isoparametric* mappings and transfinite interpolation from [30, 31]. Due to the geometry of the interface elements, we assume there is only one curved edge for each triangular and quadrilateral sub-element.

2.4.1 Quadrature On Curved-Sided Triangles

Suppose on the xy-plane, an triangle denoted by $A_1A_2A_3$ has one curved edge A_3A_1, as shown on the left in the Figure 2.4. Let the parametric equation of the curve A_3A_1 be $\Gamma(\eta) = (x(\eta), y(\eta))^T$, $\eta \in [0, 1]$. Let the direction of $\Gamma(\eta)$ be from A_1 to A_3, i.e. $\Gamma(0) = A_1$ and $\Gamma(1) = A_3$. A mapping $\mathbf{T}$ from the standard reference straight-sided triangle on $\xi\eta$-plane to the curved-sided triangle on xy-plane is given by

$$\mathbf{T}(\xi, \eta) = A_1 + (A_2 - A_1)\xi + (A_3 - A_1)\eta + \frac{1 - \xi - \eta}{1 - \eta}\left[\Gamma(\eta) - A_1 - (A_3 - A_1)\eta\right]. \quad (2.33)$$

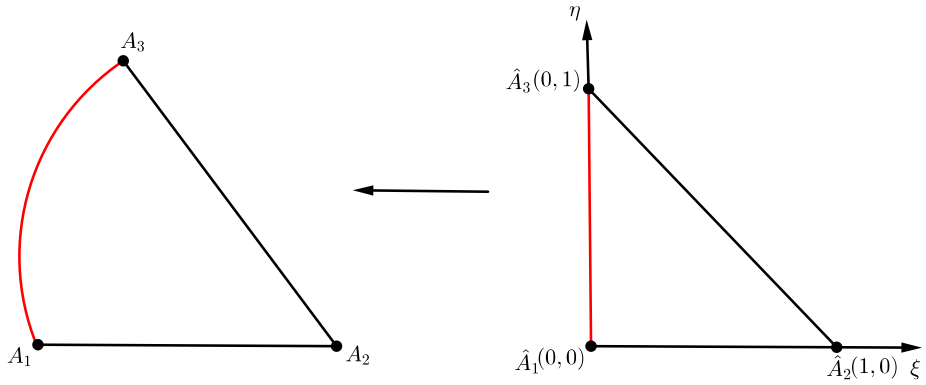

Figure 2.4: Mapping the reference triangle in the $\xi\eta$-plane to the curved-sided triangle in the xy-plane

Let $\hat{A}_1 = (0, 0)$, $\hat{A}_2 = (1, 0)$, $\hat{A}_3 = (0, 1)$. One can easily check that

$$\mathbf{T}(\xi, 0) = (1 - \xi)\Gamma(0) + \xi A_2 = (1 - \xi)A_1 + \xi A_2,$$
$$\mathbf{T}(0, \eta) = \Gamma(\eta),$$

$$\mathbf{T}(\xi, 1-\xi) = \xi A_2 + (1-\xi)A_3,$$

which show that $\mathbf{T}$ maps $\hat{A}_i\hat{A}_j$ to A_iA_j, $i \neq j$. Now suppose the integrand is $F(x, y)$. Then we have

$$\int_{A_1A_2A_3} F(x, y)dxdy = \int_{\hat{A}_1\hat{A}_2\hat{A}_3} F(\mathbf{T}(\xi, \eta))|J(\xi, \eta)|d\xi d\eta \tag{2.35}$$

where $J(\xi, \eta)$ is the Jacobian matrix of the transformation (2.33). Thus we could use the gaussian quadrature on the reference element $\hat{T} = \triangle\hat{A}_1\hat{A}_2\hat{A}_3$ and the formula (2.35) to compute the numerical integration of F on the curve-sided triangle.

2.4.2 Quadrature On Curved-Sided Quadrilateral

Similarly, suppose the quadrilateral on the xy-plane denoted by $A_1A_2A_3A_4$ has one curved side A_4A_1, as shown by Figure 2.5. The parametric equation of the curve A_4A_1 is $\Gamma(\eta)$, $\eta \in [0, 1]$ and $\Gamma(0) = A_1$, $\Gamma(1) = A_4$.

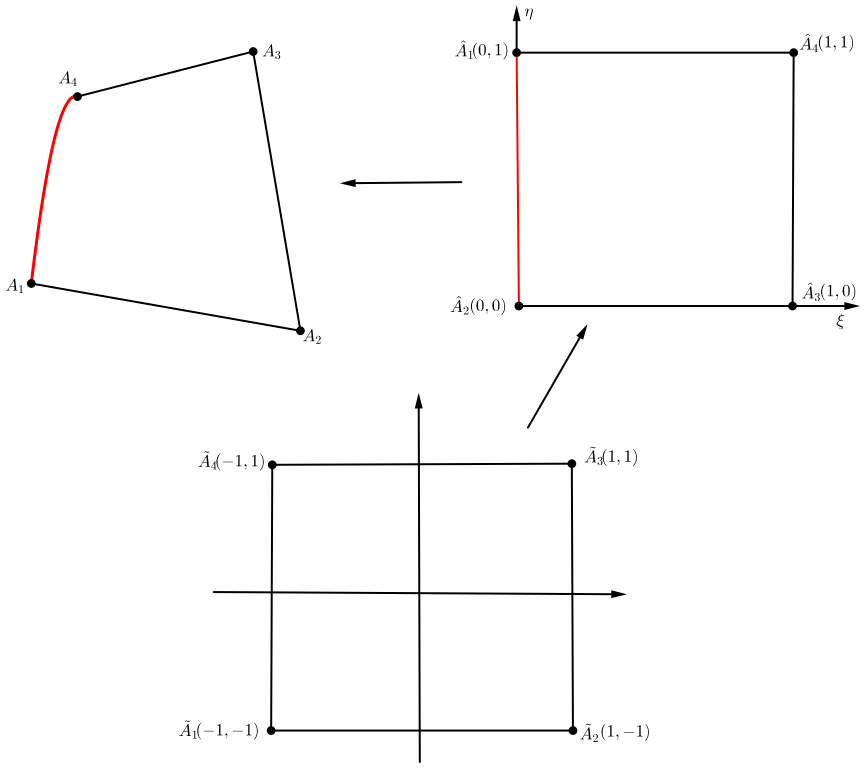

Figure 2.5: Mapping the reference quadrilateral in the $\xi\eta$-plane to the curved-sided quadrilateral in the xy-plane

In this case, the transformation is given by

$$\begin{aligned}\mathbf{T}(\hat{\xi},\hat{\eta}) &= (1-\hat{\xi})\Gamma(\hat{\eta}) + \hat{\xi}(A_2 + (A_3 - A_2)\hat{\eta}) \\ &\quad + (1-\hat{\eta})(A_1 + (A_2 - A_1)\hat{\xi}) + \hat{\eta}(A_4 + (A_3 - A_4)\hat{\xi}) \\ &\quad - ((1-\hat{\xi})((1-\hat{\eta})A_1 + \hat{\eta}A_4) + \hat{\xi}((1-\hat{\eta})A_2 + \hat{\eta}A_3))\end{aligned} \tag{2.36}$$

which mappings the square $[0,1]\times[0,1]$ in the $\hat{\xi}\hat{\eta}$-plane to the curved-sided quadrilateral. To apply the gaussian quadrature, we need another transformation for the square $[-1,1]\times[-1,1]$ to $[0,1]\times[0,1]$, i.e.

$$\hat{\xi} = \frac{1+\xi}{2}, \qquad \hat{\eta} = \frac{1+\eta}{2}. \tag{2.37}$$

Therefore, the quadrature formula is given by

$$\int_{A_1A_2A_3A_4} F(x,y)dxdy = \int_{\hat{A}_1\hat{A}_2\hat{A}_3\hat{A}_4} F\left(\mathbf{T}(\frac{1+\xi}{2},\frac{1+\eta}{2})\right)|J(\xi,\eta)|d\xi d\eta \tag{2.38}$$

where J is the Jacobian matrix of the composition of (2.36) and (2.37).

Chapter 3

A IFE Space on Triangular Mesh

In this chapter, we construct a linear IFE space $S_h(\Omega)$ on a triangular mesh formed by only the right-angle equilateral triangles, which is mostly used in the IFE method. In Section 3.1, we develop the explicit formula of the IFE shape functions and show the unisolvence and boundedness by the *Sherman-Morrison* formula. In Section 3.2 we present a group of identities for the IFE shape functions which are critical ingredients in the analysis of the interpolation errors. In Section 3.3, we show the optimal approximation capability for the constructed IFE space by combining the generalized Multi-point Taylor expansion and the fundamental identities. In Section 3.4, numerical results are given to confirm the optimal convergence rate of the interpolation errors.

Without loss of generality, we could consider the typical element:

$$A_1(0,0) \quad A_2(h,0) \quad A_3(0,h). \tag{3.1}$$

Recall the linear finite elements (T, Π_T, Σ_T^P):

$$\Pi_T = \text{Span}\{1, x, y\}, \tag{3.2a}$$

$$\Sigma_T^P = \{\psi_T(A_i) : i \in \mathcal{I},\ \forall \psi_T \in \Pi_T\}, \tag{3.2b}$$

where the supscript P is used to emphasize that the degrees of freedom are imposed pointwisely on the vertices, i.e., we consider the Lagrangian type of shape functions. And on any element T, the standard finite element shape functions are denoted by $\psi_{i,T}^P$, $i \in \mathcal{I}$:

$$\psi_{1,T}^P(X) = 1 - \frac{x}{h} - \frac{y}{h}, \tag{3.3a}$$

$$\psi_{2,T}^P(X) = \frac{x}{h}, \tag{3.3b}$$

$$\psi_{3,T}^P(X) = \frac{y}{h}. \tag{3.3c}$$

We refer readers to [8, 13, 15, 44] that the shape functions have the following well-known properties:

$$\psi_{i,T}^P(A_j) = \delta_{ij}, \quad \left\|\psi_{i,T}^P\right\|_{\infty,T} \leq C, \quad \left\|\nabla\psi_{i,T}^P\right\|_{\infty,T} \leq Ch^{-1}, \ \ i,j \in \mathcal{I}, \tag{3.4}$$

where δ_{ij} is the *Kronecker* delta function. Then the local IFE spaces on every non-interface elements T can be natruaily defined as

$$S_h^n(T) = \text{Span}\{\psi_{i,T}^P : \ i \in \mathcal{I}\}. \tag{3.5}$$

3.1 Local IFE Spaces $S_h^i(T)$ On Interface Elements

In this section, we first derive the format for the Lagrange type IFE shape functions on interface elements, $T \in \mathcal{T}_h^i$. According to [36], there are two cases of in interface elements, as shown by the Figure 3.1.

Case 1 The interface Γ cuts the adjacent edges of the right angle.

Case 2 The interface Γ cuts the adjacent edges of the non-right angle.

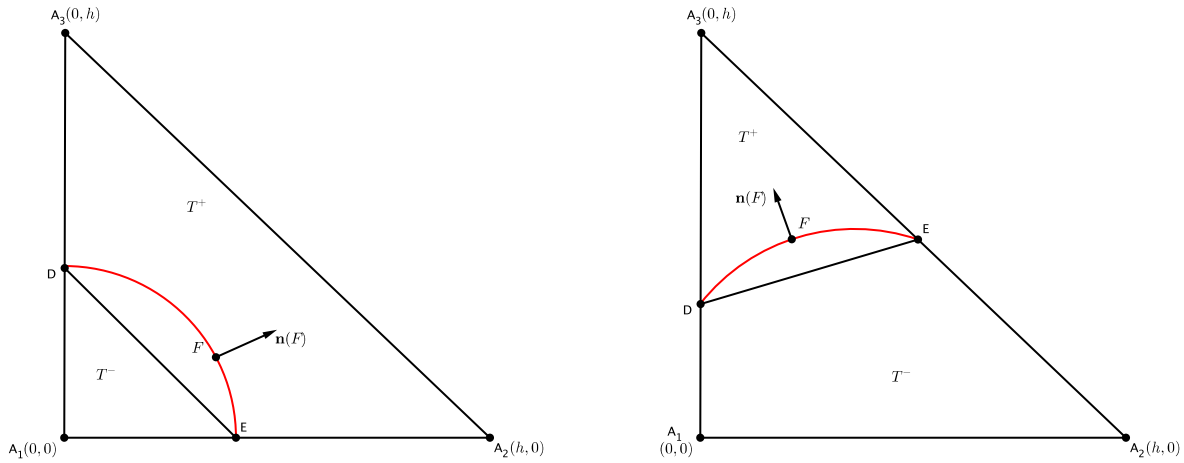

(a) Case 1 (b) Case 2

Figure 3.1: The Geometry of Triangular Interface Elements

On each interface element, we consider the following piecewise linear polynomials:

$$\phi_T^P = \begin{cases} \phi_T^{P\,-}(X) = \phi_T^-(X) \in \Pi_T, & \text{if} \quad X \in T^-, \\ \phi_T^{P\,+}(X) = \phi_T^+(X) \in \Pi_T, & \text{if} \ \ X \in T^+. \end{cases} \tag{3.6}$$

Let F be an arbitrary point on the curve. We emphasize that once F is chosen then it should be fixed for each interface element. Also let l be the straight line connecting D and E. Due to the geometry of the interface curve, it is impossible for piecewise linear polynomials to satisfy the conditions (1.3a) and (1.3b) exactly on a generic curve. So we would like to consider the following weak jump conditions:

$$\phi_T^- \in \Pi_T, \quad \text{and} \quad \phi_T^+ \in \Pi_T, \tag{3.7a}$$

$$\phi_T^-|_l = \phi_T^+|_l, \tag{3.7b}$$

$$\beta^- \nabla \phi_T^-(F) \cdot \mathbf{n}(F) = \beta^+ \nabla \phi_T^+(F) \cdot \mathbf{n}(F). \tag{3.7c}$$

We also impose the following nodal conditions:

$$\phi_T^P(A_i) = v_i, \quad i \in \mathcal{I}. \tag{3.8}$$

We need to show for any (v_1, v_2, v_3), there exists a unique ϕ_T^P which has the form (3.6) satisfying (3.7a)-(3.7c) and (3.8). Define the function $L(X)$ as

$$L(X) = \mathbf{n}(l) \cdot (X - D), \tag{3.9}$$

such that $L(X) = 0$ is the equation of the line l. The basic idea to construct the shape functions is that on one piece, we express ϕ_T^P as a linear combination of the standard finite element shape functions $\psi_{i,T}^P$ and use (3.7b) to express the format on the other piece. And without loss of generality, we can assume $|\mathcal{I}^-| \leqslant |\mathcal{I}^+|$. Then the IFE shape functions formed by piecewise polynomials can be expressed as

$$\phi_T^P(X) = \begin{cases} \phi_T^{P\,-}(X) = \phi_T^{P\,+}(X) + c_0 L(X), & if \;\; X \in T^-, \\ \phi_T^{P\,+}(X) = \displaystyle\sum_{i \in \mathcal{I}^-} c_i \psi_{i,T}^P(X) + \sum_{i \in \mathcal{I}^+} v_i \psi_{i,T}^P(X), & if \;\; X \in T^+. \end{cases} \tag{3.10}$$

It is easy to see that (3.10) satisfies the vertices condition (3.8) on T^+. So now we need to determine the coefficients c_0 and c_i, $i \in \mathcal{I}^-$ by using the nodal conditions (3.8) on T^- and the jump conditions (3.7c), which gives the following lemma.

Lemma 3.1. *For sufficiently small h, assume the formulation* (3.10) *satisfies* (3.7a)-(3.7c) *and* (3.8)*, then the unknown coefficients $c = (c_i)_{i \in \mathcal{I}^-}^T$ satisfy the following equation*

$$(I + k\, \delta \gamma^T) c = b, \tag{3.11}$$

where

$$k = \left(\frac{1}{\rho} - 1 \right) \frac{1}{\nabla L \cdot \mathbf{n}(F)} \tag{3.12}$$

is a constant and

$$\gamma = \left(\nabla \psi_{i,T}^P(F) \cdot \mathbf{n}(F) \right)_{i \in \mathcal{I}^-}^T, \tag{3.13a}$$

$$\delta = (L(A_i))_{i\in\mathcal{I}^-}^T , \tag{3.13b}$$

and

$$b = \left(v_i - kL(A_i) \sum_{j\in\mathcal{I}^+} \nabla\psi_{j,T}^P(F)\cdot\mathbf{n}(F)v_j \right)_{i\in\mathcal{I}^-}^T \tag{3.14}$$

are all column vectors. In addition, c_0 can be represented by

$$c_0 = k\left(\sum_{i\in\mathcal{I}^-} c_i \nabla\psi_{i,T}^P(F)\cdot\mathbf{n}(F) + \sum_{i\in\mathcal{I}^+} v_i \nabla\psi_{i,T}^P(F)\cdot\mathbf{n}(F) \right). \tag{3.15}$$

Proof. First note that Remark 2.1 implies

$$\nabla L\cdot\mathbf{n}(F) = \bar{\mathbf{n}}\cdot\mathbf{n}(F) \geqslant 1 - Ch^2 > 0, \tag{3.16}$$

if h is small enough. So k in (3.12) is well defined for sufficiently small h. And by applying the condition (3.7c) on (3.10), it is easy to derive the formula (3.15). Now substituting (3.15) into the first equation of (3.10) and using $\phi_T^{P\,-}(A_j) = v_j$ for any $j\in\mathcal{I}^-$, we have

$$\begin{aligned} &\sum_{i\in\mathcal{I}^-} \left(\psi_{i,T}^P(A_j) + k\nabla\psi_{i,T}^P(F)\cdot\mathbf{n}(F)L(A_j)\right) c_i \\ =&v_j - \sum_{i\in\mathcal{I}^+} \left(\psi_{i,T}^P(A_j) + k\nabla\psi_{i,T}^P(F)\cdot\mathbf{n}(F)L(A_j)\right) v_i. \end{aligned} \tag{3.17}$$

Note that $\psi_{i,T}^P(A_j) = \delta_{ij}$, for $i,j\in\mathcal{I}^-$. So (3.17) gives the linear system (3.11). □

Remark 3.1. *Since we first represent ϕ_T^P by a linear combination of $\psi_{i,T}^P$ on the piece which contains most of the vertices, there will be fewer unknown coefficients in the linear system* (3.11).

The following two lemmas are useful to show the unisolvence of (3.11).

Lemma 3.2. *Let $\bar{\gamma} = (\nabla\psi_{i,T}(F)\cdot\bar{\mathbf{n}})_{i\in\mathcal{I}^-}^T$, then*

$$k\gamma^T\delta > k\bar{\gamma}^T\delta - Ch, \tag{3.18}$$

where C only depends on ρ and the curvature of the curve.

Proof. First note that

$$|L(A_i)| \leqslant \|\bar{\mathbf{n}}\|\,\|A_i - D\| \leqslant Ch, \qquad \forall i\in\mathcal{I}^-. \tag{3.19}$$

Besides, Remark 2.1 shows that $\|\mathbf{n}(F)-\bar{\mathbf{n}}\| < Ch$ and (3.12) implies $k < C$ for some constant C. Hence by the boundedness of $\psi_{i,T}^P$, we have

$$\begin{aligned} k\gamma^T\delta =& k\sum_{i\in\mathcal{I}^-} \nabla\psi_{i,T}^P(F)\cdot\mathbf{n}(F)L(A_i) \\ =& k\sum_{i\in\mathcal{I}^-} \nabla\psi_{i,T}^P(F)\cdot\bar{\mathbf{n}}L(A_i) + k\nabla\psi_{i,T}^P(F)\cdot(\bar{\mathbf{n}}-\mathbf{n}(F))L(A_i) \\ >& k\bar{\gamma}^T\delta - Ch. \end{aligned}$$

□

Lemma 3.3. *For the two cases of interface elements, we have* $\bar{\gamma}^T\delta \in [0,1]$.

Proof. We consider the two cases individually.
Case 1. We have $\mathcal{I}^- = \{1\}$ and $\mathcal{I}^- = \{2,3\}$. Let $D = (0, hd)$ and $E = (he, 0)$ for some $d \in [0,1]$, $e \in [0,1]$ and thus, $\bar{\mathbf{n}} = (d,e)/\sqrt{e^2+d^2}$, where e and d can not be both 0 or 1 according to the hypothesis **(H1)** and the definition of the interface element. By direct calculation, one can verify that

$$\bar{\gamma}^T\delta = \nabla\psi_{1,T}^P(F)\cdot\bar{\mathbf{n}}\ L(A_1) = \frac{(e+d)de}{e^2+d^2} \in [0,1].$$

Case 2. We have $\mathcal{I}^- = \{3\}$ and $\mathcal{I}^- = \{1,2\}$. Let $D = (0, hd)$ and $E = (h-he, he)$ for some $d \in [0,1]$, $e \in [0,1]$ and thus, $\bar{\mathbf{n}} = (d-e, 1-e)/\sqrt{(d-e)^2+(1-e)^2}$, where similarly, e and d can not be both 0 or 1. By direct calculation, one can verify that

$$\bar{\gamma}^T\delta = \nabla\psi_{3,T}^P(F)\cdot\bar{\mathbf{n}}\ L(A_3) = \frac{(1-d)(1-e)^2}{\sqrt{(d-e)^2+(1-e)^2}} \in [0,1].$$

□

Lemma 3.4. *There exists a constant C independent of the interface location such that*

$$1 + k\,\gamma^T\delta > \min\left(1, \frac{1}{\rho} - Ch^2\right) - Ch. \tag{3.20}$$

Proof. Note that Lemma 3.3 yields

$$k\,\bar{\gamma}^T\delta \geqslant 0, \qquad \text{if } \ \rho \leqslant 1, \tag{3.21a}$$

$$k\,\bar{\gamma}^T\delta \geqslant \left(\frac{1}{\rho} - 1\right)\frac{1}{1-Ch^2}, \qquad \text{if } \ \rho > 1. \tag{3.21b}$$

Hence combining (3.21) and Lemma 3.2, we have (3.20). □

Theorem 3.1 (**Unisolvency**). *Given any $v = (v_1, v_2, v_3) \in \mathbb{R}^3$, for sufficiently small h, there exists a unique shape function ϕ_T^P given by* (3.10) *satisfying* (3.7a)-(3.7c) *and* (3.8).

Proof. Due to the special structure of (3.11), by the *Sherman-Morrison* formula, it has a unique solution if and only if $1 + k\gamma^T\delta \neq 0$. Indeed, Lemma 3.4 shows that it has a uniform positive lower bound provided h is small enough, which yields the unisolvence. □

By the *Sherman-Morrison* formula again, the solution to (3.11) can be explicitly computed as

$$c = b - k\frac{(\gamma^T b)\delta}{1 + k\gamma^T\delta}. \tag{3.22}$$

Now we consider $v = (1, 0, 0)^T$, $(0, 1, 0)^T$ and $(0, 0, 1)^T$ in Theorem 3.1, which gives the IFE shape functions $\phi_{i,T}^P$, $i \in \mathcal{I}$, satisfying

$$\phi_{i,T}^P(A_j) = \delta_{ij}, \quad i, j \in \mathcal{I}. \tag{3.23}$$

And the local IFE spaces $S_h^i(T)$ on interface elements $T \in \mathcal{T}_h^i$ are given by

$$S_h^i(T) = \text{Span}\{\phi_{i,T}^P : \ i = 1, 2, 3\}. \tag{3.24}$$

By making the shape functions continuous at the nodes of the mesh, the global IFE space $S_h(\Omega)$ can be defined as

$$\begin{aligned} S_h(\Omega) = \big\{ & v \in L^2(\Omega) : v|_T \in S_h^n(T) \text{ if } T \in \mathcal{T}_h^n, \ v|_T \in S_h^i(T) \text{ if } T \in \mathcal{T}_h^i; \\ & \text{if } T_1 \cap T_2 = A \in \mathcal{N}_h, \text{ then } v|_{T_1}(A) = v|_{T_2}(A) \big\}. \end{aligned} \tag{3.25}$$

3.2 Properties of IFE Shape Functions

In this section, we present some important properties of the IFE shape functions which are very useful in the analysis of interpolation errors. First, we can easily show the boundedness of the IFE shape functions (3.23) by using the *Sherman-Morrison* formula (3.22).

Theorem 3.2 (Boundedness of IFE Shape functions). *Given any $T \in \mathcal{T}_h^i$, for sufficiently small h, there exist constants C, independent of the interface location, such that for $i \in \mathcal{I}$, we have*

$$|\phi_{i,T}^P|_{k,\infty,T} \leqslant Ch^{-k}, \quad k = 0, 1. \tag{3.26}$$

Proof. Since $|\psi_{i,T}^P|_{k,\infty,T} \leqslant Ch^{-k}$, $i \in \mathcal{I}$, we only need to prove the coefficients in (3.10) are uniformly bounded. Note that $\|\nabla\psi_{i,T}^P\|_{\infty,T} \leqslant Ch^{-1}$, $i \in \mathcal{I}$, $\|L\|_{\infty,T} < Ch$ and $k < C$. So we have, $\|\gamma\| < Ch^{-1}$, $\|\delta\| < Ch$ and $\|b\| < C$. Hence (3.22) and (3.4) imply that

$$\|c\| < \|b\| + \frac{\|\gamma\|\|b\|\|\delta\|}{\min\left(1, \frac{1}{\rho} - Ch^2\right) - Ch} < C.$$

Besides, (3.15) shows $|c_0| \leqslant Ch^{-1}$. Finally we have $\|c_0 L\|_{\infty,T} \leqslant C$ and $\|c_0 \nabla L\|_{\infty,T} \leqslant C$ by $\|L\|_{\infty,T} < Ch$ and $\|\nabla L\|_{\infty,T} < C$. □

Next we show that the IFE shape functions inherit the partition of utility from the standard IFE shape functions.

Lemma 3.5 (Partition of Utility)**.** *Let $\phi_{i,T}^P$, $i \in \mathcal{I}$, be the IFE shape functions given by* (3.23)*, then*

$$\sum_{i\in\mathcal{I}} \phi_{i,T}^P(X) \equiv 1, \tag{3.27}$$

$$\nabla\left(\sum_{i\in\mathcal{I}} \phi_{i,T}^P(X)\right) = \sum_{i\in\mathcal{I}} \nabla\phi_{i,T}^P(X) \equiv 0. \tag{3.28}$$

Proof. Denote the right hand of (3.27) by $\phi(X)$. Note that $\phi \in S_h^i(T)$ and $\phi(A_i) = 1$, $i \in \mathcal{I}$. So (3.27) follows from the unisolvency directly. And (3.28) is simply the consequence of (3.27). □

Now we consider the following two vector functions:

$$\Lambda_1(X) = \sum_{i\in\mathcal{I}} (A_i - X)\phi_{i,T}^{P,+}(X) + \sum_{i\in\mathcal{I}^-} (\overline{M}^+(F) - I)^T (A_i - \overline{X}_i)\phi_{i,T}^{P,+}(X), \quad \text{if } X \in T^+, \tag{3.29a}$$

$$\Lambda_2(X) = \sum_{i\in\mathcal{I}} (A_i - X)\phi_{i,T}^{P,-}(X) + \sum_{i\in\mathcal{I}^+} (\overline{M}^-(F) - I)^T (A_i - \overline{X}_i)\phi_{i,T}^{P,-}(X), \quad \text{if } X \in T^-, \tag{3.29b}$$

where $\overline{X}_i$ are arbitrary points on l. It follows from the Lemma 2.5 that the two functions in (3.29a) and (3.29b) are independent of location of $\overline{X}_i$, i.e., they are well defined. Note that $\phi_{i,T}^{P,+}(X) \in \Pi_T$, for $i \in \mathcal{I}$. And from the partition of utility, we have

$$\Lambda_1(X) = \sum_{i\in\mathcal{I}} A_i\phi_{i,T}^{P,+}(X) - X + \sum_{i\in\mathcal{I}^-} (\overline{M}^+(F) - I)^T (A_i - \overline{X}_i)\phi_{i,T}^{P,+}(X), \tag{3.30a}$$

$$\Lambda_2(X) = \sum_{i\in\mathcal{I}} A_i\phi_{i,T}^{P,-}(X) - X + \sum_{i\in\mathcal{I}^+} (\overline{M}^-(F) - I)^T (A_i - \overline{X}_i)\phi_{i,T}^{P,-}(X). \tag{3.30b}$$

Thus each component of $\Lambda_1(X)$ and $\Lambda_2(X)$ is in Π_T. Now we can define the following two vector functions

$$\Lambda^+(X) = \Lambda_1(X), \quad \text{and} \quad \Lambda^-(X) = (\overline{M}^+)^T \Lambda_2(X). \tag{3.31}$$

The following properties show that $\Lambda^+(X)$ and $\Lambda^-(X)$ actually form a piecewise polynomial in $S_h^i(T)$.

Lemma 3.6. Λ^+ *and* Λ^- *satisfy the condition* (3.7a)*, i.e. each component is in* Π_T*.*

Proof. Note that $(\overline{M}^+(F))^T$ is a constant matrix. So the result follows directly from the fact that each component of Λ_i, $i = 1, 2$ is in Π_T. □

Lemma 3.7. Λ^+ *and* Λ^- *satisfy the condition* (3.7b)*, i.e.* $\Lambda^+(X)|_l = \Lambda^-(X)|_l$*.*

Proof. For any point $\overline{X}$ on l, we can take $\overline{X}_i = \overline{X}$ in both the (3.29a) and (3.29b). Since $\phi^P_{i,T}$ satisfies (3.7b), we have

$$\begin{aligned}\Lambda^+(\overline{X}) =& \sum_{i\in\mathcal{I}}(A_i - \overline{X})\phi^{P-}_{i,T}(\overline{X}) + \sum_{i\in\mathcal{I}^-}(\overline{M}^+(F) - I)^T(A_i - \overline{X})\phi^{P-}_{i,T}(\overline{X})\\ =& \sum_{i\in\mathcal{I}^+}(A_i - \overline{X})\phi^{P-}_{i,T}(\overline{X}) + (\overline{M}^+(F))^T\sum_{i\in\mathcal{I}^-}(A_i - \overline{X})\phi^{P-}_{i,T}(\overline{X}).\end{aligned}$$

And from (2.15), one can verify that

$$\begin{aligned}\Lambda^+(\overline{X}) &= (\overline{M}^+(F))^T\left((\overline{M}^-(F))^T\sum_{i\in\mathcal{I}^+}(A_i - \overline{X})\phi^{P-}_{i,T}(\overline{X}) + \sum_{i\in\mathcal{I}^-}(A_i - \overline{X})\phi^{P-}_{i,T}(\overline{X})\right)\\ &= (\overline{M}^+(F))^T\left((\overline{M}^-(F) - I)^T\sum_{i\in\mathcal{I}^+}(A_i - \overline{X})\phi^{P-}_{i,T}(\overline{X}) + \sum_{i\in\mathcal{I}}(A_i - \overline{X})\phi^{P-}_{i,T}(\overline{X})\right),\end{aligned}$$

which is exactly $\Lambda^-(\overline{X})$. □

Lemma 3.8. Λ^+ *and* Λ^- *satisfy the condition* (3.7c)*, i.e.* $\beta^+\nabla\Lambda^+(F)\cdot\mathbf{n}(F) = \beta^-\nabla\Lambda^-(F)\cdot\mathbf{n}(F)$*, where the gradient operator is understood as the gradient on each component.*

Proof. Similarly we can take $\overline{X}_i$ to be an arbitrary point $\overline{X}$. Since $\phi^T_{i,T}$ satisfies (3.7c), we have

$$\begin{aligned}&\beta^+\nabla\Lambda^+(F)\cdot\mathbf{n}(F)\\ =&\sum_{i\in\mathcal{I}}A_i\beta^-\nabla\phi^{P-}_{i,T}(F)\cdot\mathbf{n}(F)\\ &+(\overline{M}^+(F) - I)^T\sum_{i\in\mathcal{I}^-}(A_i - \overline{X})\beta^-\nabla\phi^{P-}_{i,T}(F)\cdot\mathbf{n}(F) - \beta^+\mathbf{n}(F)\end{aligned}$$

Then from Lemma (3.5) and (2.15), we have

$$
\begin{aligned}
&\sum_{i\in\mathcal{I}} A_i\beta^-\nabla\phi_{i,T}^{P,-}(F)\cdot\mathbf{n}(F) + (\overline{M}^+(F)-I)^T\sum_{i\in\mathcal{I}^-}(A_i-\overline{X})\beta^-\nabla\phi_{i,T}^{P,-}(F)\cdot\mathbf{n}(F)\\
=&\sum_{i\in\mathcal{I}^+} A_i\beta^-\nabla\phi_{i,T}^{P,-}(F)\cdot\mathbf{n}(F) + \sum_{i\in\mathcal{I}^-}\overline{X}\beta^-\nabla\phi_{i,T}^{P,-}(F)\cdot\mathbf{n}(F)\\
&+(\overline{M}^+(F))^T\sum_{i\in\mathcal{I}^-}(A_i-\overline{X})\beta^-\nabla\phi_{i,T}^{P,-}(F)\cdot\mathbf{n}(F)\\
=&\sum_{i\in\mathcal{I}^+}(A_i-\overline{X})\beta^-\nabla\phi_{i,T}^{P,-}(F)\cdot\mathbf{n}(F) + (\overline{M}^+(F))^T\sum_{i\in\mathcal{I}^-}(A_i-\overline{X})\beta^-\nabla\phi_{i,T}^{P,-}(F)\cdot\mathbf{n}(F)\\
=&(\overline{M}^+(F))^T\left((\overline{M}^-(F))^T\sum_{i\in\mathcal{I}^+}(A_i-\overline{X})\beta^-\nabla\phi_{i,T}^{P,-}(F)\cdot\mathbf{n}(F) + \sum_{i\in\mathcal{I}^-}(A_i-\overline{X})\beta^-\nabla\phi_{i,T}^{P,-}(F)\cdot\mathbf{n}(F)\right)\\
=&(\overline{M}^+(F))^T\left(\sum_{i\in\mathcal{I}}(A_i-\overline{X})\beta^-\nabla\phi_{i,T}^{P,-}(\overline{X}) + \sum_{i\in\mathcal{I}^+}(\overline{M}^-(F)-I)^T(A_i-\overline{X})\beta^-\nabla\phi_{i,T}^{P,-}(\overline{X})\right).
\end{aligned}
$$

Finally according to (2.16), we have $\beta^-(\overline{M}^+(F))^T\mathbf{n}(F)=\beta^+\mathbf{n}(F)$ and

$$
\begin{aligned}
&\beta^+\nabla\Lambda^+(F)\cdot\mathbf{n}(F)\\
=&(\overline{M}^+(F))^T\left(\sum_{i\in\mathcal{I}}(A_i-\overline{X})\beta^-\nabla\phi_{i,T}^{P,-}(\overline{X}) + \sum_{i\in\mathcal{I}^+}(\overline{M}^-(F)-I)^T(A_i-\overline{X})\beta^-\nabla\phi_{i,T}^{P,-}(\overline{X}) - \beta^-\mathbf{n}(F)\right)\\
=&\beta^-\nabla\Lambda^-(F)\cdot\mathbf{n}(F),
\end{aligned}
$$

which finishes the proof. □

Theorem 3.3. *On each interface element T, the IFE shape functions satisfy*

$$\sum_{i\in\mathcal{I}}(A_i-X)\phi_{i,T}^{P,+}(X) + \sum_{i\in\mathcal{I}^-}(\overline{M}^+(F)-I)^T(A_i-\overline{X}_i)\phi_{i,T}^{P,+}(X)\equiv 0, \tag{3.32a}$$

$$\sum_{i\in\mathcal{I}}(A_i-X)\phi_{i,T}^{P,-}(X) + \sum_{i\in\mathcal{I}^+}(\overline{M}^-(F)-I)^T(A_i-\overline{X}_i)\phi_{i,T}^{P,-}(X)\equiv 0. \tag{3.32b}$$

Proof. We define a piecewise vector function on T as

$$\Lambda(X)=\begin{cases}\Lambda^+(X), & \text{if } X\in T^+,\\ \Lambda^-(X), & \text{if } X\in T^-.\end{cases}$$

The Lemmas 3.6, 3.7 and 3.8 show that each component of Λ satisfies the conditions (3.7a)-(3.7c) that is, each component of Λ is in $S_h^i(T)$. And we note that $\Lambda(A_i)=0$, $i\in\mathcal{I}$. Therefore, from the unisolvency, we have $\Lambda^+(X)=\Lambda_1(X)\equiv 0$ and $\Lambda^-(X)=(\overline{M}^+(F))^T\Lambda_2(X)\equiv 0$, for any $X\in T$. Since $(\overline{M}^+(F))^T$ is nonsingular, we have $\Lambda_2(X)\equiv 0$. □

Theorem 3.4. *On each interface element T, we have*

$$\sum_{i\in\mathcal{I}}(A_i - X)\partial_x\phi_{i,T}^{P\,+}(X) + \sum_{i\in\mathcal{I}^-}\left[(\overline{M}^+(F) - I)^T(A_i - \overline{X}_i)\partial_x\phi_{i,T}^{P\,+}(X)\right] - \mathbf{e}_1 \equiv 0, \tag{3.33a}$$

$$\sum_{i\in\mathcal{I}}(A_i - X)\partial_y\phi_{i,T}^{P\,+}(X) + \sum_{i\in\mathcal{I}^-}\left[(\overline{M}^+(F) - I)^T(A_i - \overline{X}_i)\partial_y\phi_{i,T}^{P\,+}(X)\right] - \mathbf{e}_2 \equiv 0. \tag{3.33b}$$

and

$$\sum_{i\in\mathcal{I}}(A_i - X)\partial_x\phi_{i,T}^{P\,-}(X) + \sum_{i\in\mathcal{I}^+}\left[(\overline{M}^-(F) - I)^T(A_i - \overline{X}_i)\partial_x\phi_{i,T}^{P\,-}(X)\right] - \mathbf{e}_1 \equiv 0, \tag{3.34a}$$

$$\sum_{i\in\mathcal{I}}(A_i - X)\partial_y\phi_{i,T}^{P\,-}(X) + \sum_{i\in\mathcal{I}^+}\left[(\overline{M}^-(F) - I)^T(A_i - \overline{X}_i)\partial_y\phi_{i,T}^{P\,-}(X)\right] - \mathbf{e}_2 \equiv 0. \tag{3.34b}$$

where $\mathbf{e}_1 = (1,0)^T$, $\mathbf{e}_2 = (0,1)^T$.

Proof. (3.33) and (3.34) can be verified by direct differentiating (3.32a) and (3.32b). □

3.3 Approximation Capabilities

In this section, we discuss the approximation capabilities of the IFE space $S_h(\Omega)$ on a triangular partition $\mathcal{T}_h$. We inherit the notation $\mathcal{I}$, $\mathcal{I}^+$ and $\mathcal{I}^-$ from the last section. For $T \in \mathcal{T}_h^n$, the standard interpolation operator $I_h, T : H^2(T) \to S_h^n(T)$ is defined as:

$$I_{h,T}u = \sum_{i\in\mathcal{I}} u(A_i)\psi_{i,T}^P, \tag{3.35}$$

where A_i, $i \in \mathcal{I}$ are the vertices of T. And we define the interpolation operator on an interface element T as $I_{h,T} : PH_{int}^2(T) \to S_h^i(T)$ by

$$I_{h,T}u = \sum_{i\in\mathcal{I}} u(A_i)\phi_{i,T}^P. \tag{3.36}$$

So the global IFE interpolation $I_h : PH_{int}^2(\Omega) \to S_h(\Omega)$ can be defined as

$$(I_h u)|_T = I_{h,T}u, \quad \forall T \in \mathcal{T}_h. \tag{3.37}$$

For any non-interface element T, according to the standard scaling argument in [11], we have

$$\|I_{h,T}u - u\|_{0,T} + h\|I_{h,T}u - u\|_{1,T} \leqslant Ch^2|u|_{2,T}. \tag{3.38}$$

However on an interface element T, since $S_h^i(T)$ is not even contained in $H^1(T)$, how to apply the standard scaling argument in this situation is not clear. In the following discussion, we

use the multi-point Taylor expansions given by (2.19) and (2.22) to derive the interpolation error.

Without loss of generality, we assume the interface T has the configuration illustrated in Figure 2.3, and all the discussion in this section are based on $X \in T^+$. For any $i \in \mathcal{I}$, we let $Y_i(t, X) = tA_i + (1-t)X$. And for $i \in \mathcal{I}^-$, there is a $\tilde{t}_i \in [0, 1]$ such that $\widetilde{Y}_i = \tilde{t}_i A_i + (1-\tilde{t}_i)X$ is on the curve $\Gamma \cap T$. Then we have the following theorem to expand the interpolation error.

Theorem 3.5. *Let T be any interface element and $u \in PC^2_{int}(T)$, then for any $\overline{X}_i \in l$, $i \in \mathcal{I}^-$, we have*

$$I_{h,T}u(X) - u(X) = \sum_{i\in\mathcal{I}^-}(E_i + F_i)\phi^P_{i,T}(X) + \sum_{i\in\mathcal{I}} R_i\phi^P_{i,T}(X), \tag{3.39}$$

and

$$\partial_s(I_{h,T}u(X) - u(X)) = \sum_{i\in\mathcal{I}^-}(E_i + F_i)\partial_s\phi^P_{i,T}(X) + \sum_{i\in\mathcal{I}} R_i\partial_s\phi^P_{i,T}(X), \tag{3.40}$$

for $s = x$ or y, where R_i are given by (2.20) *and* (2.21) *and*

$$E_i = \Big((M^+(\widetilde{Y}_i) - \overline{M}^+(F))\nabla u^+(X)\Big)\cdot(A_i - \widetilde{Y}_i), \tag{3.41a}$$

$$F_i = -\Big((\overline{M}^+(F) - I)\nabla u^+(X)\Big)\cdot(\widetilde{Y}_i - \overline{X}_i), \quad i \in \mathcal{I}^-. \tag{3.41b}$$

Proof. Substituting the expansion (2.19) and (2.22) into the interpolation operator (3.36) yields that

$$\begin{aligned} I_{h,T}u(X) =& u^+(X)\sum_{i\in\mathcal{I}}\phi^P_{i,T}(X) + \nabla u^+(X)\cdot\sum_{i\in\mathcal{I}}(A_i - X)\phi^P_{i,T}(X) \\ &+ \sum_{i\in\mathcal{I}^-}\Big(\Big(M^+(\widetilde{Y}_i) - I\Big)\nabla u^+(X)\Big)\cdot(A_i - \widetilde{Y}_i)\phi^P_{i,T}(X) + \sum_{i\in\mathcal{I}} R_i\phi^P_{i,T}(X). \end{aligned} \tag{3.42}$$

From the Theorem 3.3, we have the following identity

$$\sum_{i\in\mathcal{I}}(A_i - X)\phi^P_{i,T}(X) = -\sum_{i\in\mathcal{I}^-}(\overline{M}^+(F) - I)^T(A_i - \overline{X}_i)\phi^P_{i,T}(X). \tag{3.43}$$

Then, substituting (3.43) into (3.42) and applying the partition of utility, we have

$$\begin{aligned} I_{h,T}u(X) =& u^+(X) - \sum_{i\in\mathcal{I}^-}\Big((\overline{M}^+(F) - I)\nabla u^+(X)\Big)\cdot(A_i - \overline{X}_i)\phi^P_{i,T}(X) \\ &+ \sum_{i\in\mathcal{I}^-}\Big(\Big(M^+(\widetilde{Y}_i) - I\Big)\nabla u^+(X)\Big)\cdot(A_i - \widetilde{Y}_i)\phi^P_{i,T}(X) + \sum_{i\in\mathcal{I}} R_i\phi_{i,T}(X). \end{aligned} \tag{3.44}$$

Next substituting $A_i - \overline{X}_i = (A_i - \widetilde{Y}_i) + (\widetilde{Y}_i - \overline{X}_i)$ into (3.44) and combining the term with $A_i - \widetilde{Y}_i$, we have

$$\begin{aligned} I_{h,T}u(X) =& u^+(X) - \sum_{i\in\mathcal{I}^-} \left((\overline{M}^-(F) - I)\nabla u^+(X) \right) \cdot (A_i - \widetilde{Y}_i)\phi_{i,T}^P(X) \\ & - \sum_{i\in\mathcal{I}^-} \left((\overline{M}^+(F) - I)\nabla u^+(X) \right) \cdot (\widetilde{Y}_i - \overline{X}_i)\phi_{i,T}^P(X) \\ & + \sum_{i\in\mathcal{I}^-} \left(\left(M^+(\widetilde{Y}_i) - I \right) \nabla u^+(X) \right) \cdot (A_i - \widetilde{Y}_i)\phi_{i,T}^P(X) + \sum_{i\in\mathcal{I}} R_i\phi_{i,T}^P(X) \\ =& u^+(X) + \sum_{i\in\mathcal{I}^-} \left(\left(M^+(\widetilde{Y}_i) - \overline{M}^+(F) \right) \nabla u^+(X) \right) \cdot (A_i - \widetilde{Y}_i)\phi_{i,T}^P(X) \\ & - \sum_{i\in\mathcal{I}^-} \left((\overline{M}^+(F) - I)\nabla u^+(X) \right) \cdot (\widetilde{Y}_i - \overline{X}_i)\phi_{i,T}^P(X) + \sum_{i\in\mathcal{I}} R_i\phi_{i,T}^P(X), \end{aligned} \tag{3.45}$$

which is exactly (3.39). For (3.40), we only consider the case $s = x$, and the argument for $s = y$ is similar. First note that the interpolation operator (3.35) gives

$$\partial_x I_{h,T}u(X) = \sum_{i\in\mathcal{I}} u(A_i)\partial_x\phi_{i,T}^P(X). \tag{3.46}$$

Similarly, substituting the expansion (2.19) and (2.22) into (3.46) leads to

$$\begin{aligned} \partial_x I_{h,T}u(X) =& u^+(X)\sum_{i\in\mathcal{I}} \partial_x\phi_{i,T}^P(X) + \nabla u^P(X) \cdot \sum_{i\in\mathcal{I}} (A_i - X)\partial_x\phi_{i,T}^P(X) \\ & + \sum_{i\in\mathcal{I}^-} \left(\left(M^+(\widetilde{Y}_i) - I \right) \nabla u^+(X) \right) \cdot (A_i - \widetilde{Y}_i)\partial_x\phi_{i,T}^P(X) + \sum_{i\in\mathcal{I}} R_i\partial_x\phi_{i,T}^P(X). \end{aligned}$$

Note that $\sum_{i\in\mathcal{I}} \partial_x\phi_{i,T}^P \equiv 0$ from (3.28). And by the similar argument above, we apply Theorem 3.33 to get

$$\begin{aligned} \partial_x I_{h,T}u(X) =& \nabla u^+(X)\cdot\mathbf{e}_1 - \sum_{i\in\mathcal{I}^-} \left(\left(\overline{M}^+(F) - I \right) \nabla u^+(X) \right) \cdot (A_i - \overline{X}_i)\partial_x\phi_{i,T}^P(X) \\ & + \sum_{i\in\mathcal{I}^-} \left(\left(M^+(\widetilde{Y}_i) - I \right) \nabla u^+(X) \right) \cdot (A_i - \widetilde{Y}_i)\partial_x\phi_{i,T}^P(X) + \sum_{i\in\mathcal{I}} R_i\partial_x\phi_{i,T}^P(X), \end{aligned}$$

where we use the fact $\nabla u^+(X)\cdot\mathbf{e}_1 = \partial_x u^+$. Then we have (3.40) by the same argument in (3.45). □

As in [36], we can estimate every term in (3.39) and (3.40) in L^2 norm. Note that the estimation of second order term in (3.39) and (3.40) are directly from Lemma 2.8-Lemma 2.10. So we only need to estimate E_i and F_i.

Lemma 3.9. *For any interface element $T \in \mathcal{T}_h^i$ and every $u \in PC_{int}^2(T)$, there exists a constant $C > 0$ independent of the interface location such that*

$$\|E_i\|_{0,T^+} \leqslant Ch^2\|u\|_{2,T^+}, \tag{3.47}$$
$$\|F_i\|_{0,T^+} \leqslant Ch^2\|u\|_{2,T^+}, \tag{3.48}$$

where $i \in \mathcal{I}^-$.

Proof. Note that $\|A_i - \widetilde{Y}_i\| \leqslant h$ and from Lemma 2.3, we have

$$\|E_i\|_{0,T^+} \leqslant \|(M^+(\widetilde{Y}_i) - \overline{M}^-(F))\|\ \|\nabla u^+\|_{0,T^+}\ \|(A_i - \widetilde{Y}_i)\| \leqslant Ch^2|u|_{2,T^+},$$

which implies (3.47). And taking $\overline{X}_i = \widetilde{Y}_{i\perp}$ and applying Lemma 2.2, we have

$$\|F_i\|_{0,T^+} \leqslant \|\overline{M}^+(F) - I\|\ \|\nabla u^+\|_{0,T^+}\ \|\widetilde{Y}_i - \widetilde{Y}_{i\perp}\| \leqslant Ch^2|u|_{2,T^+},$$

which yields (3.48). □

Now we are ready to prove the main result in this thesis.

Theorem 3.6. *For any interface element $T \in \mathcal{T}_h^i$ and for every $u \in PH_{int}^2(T)$, there exists a constant $C > 0$ independent of the interface location such that*

$$\|I_{h,T}u - u\|_{0,T^+} + h\|\partial_s(I_{h,T}u - u)\|_{0,T^+} \leqslant Ch^2\|u\|_{2,T}, \tag{3.49}$$

where $s = x$ or y.

Proof. First we assume $u \in PC_{int}^2(T)$. Then, from the Theorem 3.2 and Theorem 3.5, there exist constants C such that

$$\|I_{h,T}u - u\|_{0,T^+} \leqslant C\left(\sum_{i\in\mathcal{I}^-}(\|E_i\|_{0,T^+} + \|F_i\|_{0,T^+}) + \sum_{i\in\mathcal{I}}\|R_i\|_{0,T^+}\right), \tag{3.50}$$

$$\|\partial_s(I_{h,T}u - u)\|_{0,T^+} \leqslant \frac{C}{h}\left(\sum_{i\in\mathcal{I}^-}(\|E_i\|_{0,T^+} + \|F_i\|_{0,T^+}) + \sum_{i\in\mathcal{I}}\|R_i\|_{0,T^+}\right), \tag{3.51}$$

where $s = x$ or y. And Lemma 2.8 shows that

$$\|R_i\|_{0,T^+} \leqslant Ch^2|u|_{0,T} \quad \text{if } i \in \mathcal{I}^+. \tag{3.52}$$

Besides lemma 2.9 and Lemma 2.10 show that

$$\|R_i\|_{0,T^+} \leqslant Ch^2|u|_{0,T} \quad \text{if } i \in \mathcal{I}^-. \tag{3.53}$$

Combining (3.52), (3.53) and Lemma 3.9, we have that (3.49) is true for $u \in PC_{int}^2(T)$. Then the density hypothesis **(H4)** indicates that it is still true for any $u \in PH_{int}^2(T)$. □

Remark 3.2. *By the similar argument above, we can show the estimate in Theorem 3.6 on T^-, i.e., there is a constant $C > 0$ independent of the interface location such that*

$$\|I_{h,T}u - u\|_{0,T^-} + h\|\partial_s(I_{h,T}u - u)\|_{0,T^-} \leqslant Ch^2\|u\|_{2,T}, \tag{3.54}$$

where $s = x$ or y.

The local estimation Theorem 3.6 leads to the following global estimation directly.

Theorem 3.7. *For any $u \in PH^2_{int}(\Omega)$, the following estimate of the interpolation error holds*

$$\|I_h u - u\|_{0,\Omega} + h|I_h u - u|_{1,\Omega} \leqslant Ch^2\|u\|_{2,\Omega}. \tag{3.55}$$

Proof. Summing the estimation (3.49) and (3.38) together over all the elements, we have the global estimation. □

3.4 Numerical Examples

In this section, a group of numerical examples will be given to verify the approximation capabilities of the proposed linear IFE space $S_h(\Omega)$. Also we give two examples to report the performance of the IFE solutions, which is a topic in the future research. In the experiments, we consider the triangular mesh on a rectangular domain $\Omega = [-1, 1] \times [-1, 1]$. The interface curve Γ is a circle with radius $r_0 = \pi/6.28$ which divides Ω into two subdomains Ω^- and Ω^+ where

$$\Omega^- = \{(x, y) : x^2 + y^2 \leqslant r_0^2\}.$$

And the exact solution is given by [36]:

$$u(x, y) = \begin{cases} \dfrac{1}{\beta^-} r^\alpha, & (x, y) \in \Omega^-, \\ \dfrac{1}{\beta^+} r^\alpha + \left(\dfrac{1}{\beta^-} - \dfrac{1}{\beta^+}\right) r_0^\alpha & (x, y) \in \Omega^+, \end{cases} \tag{3.56}$$

where $r = \sqrt{x^2 + y^2}$ and $\alpha = 5$. First we show the results of the interpolation errors by two examples with moderate coefficients $\beta^- = 1$, $\beta^+ = 10$ and the challenging one $\beta^- = 1$, $\beta^+ = 10000$. In all the tables, the rate is the estimated value of the r such that $\|I_h u - u\|_{0,\Omega} = Ch^r$ and $|I_h u - u|_{1,\Omega} = Ch^r$. The Table 3.1 and Table 3.2 demonstrate the results for the interpolation errors in L^2-norm $\|I_h u - u\|_{0,\Omega}$ and semi H^1-norm $|I_h u - u|_{1,\Omega}$. For both cases, the numerical results indicate that the interpolation errors converge at the optimal rate, which agrees with the theoretical analysis in the last section.

h	$\|\cdot\|_{0,\Omega}$	rate	$\|\cdot\|_{1,\Omega}$	rate
1/10	1.5442E-2		2.1992E-1	
1/20	3.9403E-3	1.9705	1.1190E-1	0.9748
1/40	9.9324E-4	1.9881	5.6392E-2	0.9887
1/80	2.4942E-4	1.9936	2.8309E-2	0.9942
1/160	6.2514E-5	1.9963	1.4185E-2	0.9969
1/320	1.5625E-5	1.9979	7.1008E-3	0.9983
1/640	3.9155E-6	1.9990	3.5524E-3	0.9992
1/1280	9.7922E-7	1.9995	1.7767E-3	0.9996

Table 3.1: Errors of IFE interpolation $I_h u$ with $\beta^- = 1$ and $\beta^+ = 10$.

h	$\|\cdot\|_{0,\Omega}$	rate	$\|\cdot\|_{1,\Omega}$	rate
1/10	2.6058E-3		4.2946E-2	
1/20	1.0201E-3	1.3531	2.9798E-2	0.5273
1/40	2.7946E-4	1.8679	1.6005E-2	0.8967
1/80	7.3838E-5	1.9202	8.3549E-3	0.9378
1/160	1.9046E-5	1.9549	4.2793E-3	0.9653
1/320	4.8468E-6	1.9744	2.1686E-3	0.9806
1/640	1.2215E-6	1.9884	1.0912E-3	0.9909
1/1280	3.0663E-7	1.9941	5.4735E-4	0.9954

Table 3.2: Errors of IFE interpolation $I_h u$ with $\beta^- = 1$ and $\beta^+ = 10000$.

Besides we also present a group of numerical results for the IFE solution errors $u - u_h$ by using the symmetric partial penalty IFE(SPPIFE) scheme introduced by [39], i.e.,

$$\begin{aligned} a_h(u_h, v_h) = (u_h, v_h)_{L^2(\Omega)}, \quad \forall v_h \in S_h(\Omega), \\ u_h(X) = g(X), \quad \forall\ X \in \mathcal{N}_h \cap \partial\Omega, \end{aligned} \tag{3.57}$$

where

$$\begin{aligned} a_h(u_h, v_h) = \sum_{T\in\mathcal{T}_h} \int_T \beta \nabla u_h \cdot \nabla v_h dX - \sum_{B\in\mathring{\mathcal{E}}_h^i} \int_B \{\beta \nabla u_h \cdot \mathbf{n}_B\}[v_h] ds \\ - \sum_{B\in\mathring{\mathcal{E}}_h^i} \int_B \{\beta \nabla v_h \cdot \mathbf{n}_B\}[u_h] ds + \sum_{B\in\mathring{\mathcal{E}}_h^i} \frac{\sigma_B^0}{|B|} \int_B [u_h][v_h] ds, \end{aligned} \tag{3.58}$$

in which σ_B^0 is chosen to be $10 \max\{\beta^-, \beta^+\}$. Also the Tables 3.3 and 3.4 show the results of two examples: one is for moderate ratio, $\beta^- = 1$, $\beta^+ = 10$ and another one is for the large

ratio, $\beta^- = 1$, $\beta^+ = 10000$. As we can see from the tables, the SPPIFE solutions also have the optimal convergence rate in L^2-norm and semi H^1-norm.

h	$\|\cdot\|_{\infty,\Omega}$	rate	$\|\cdot\|_{0,\Omega}$	rate	$\|\cdot\|_{1,\Omega}$	rate
1/10	6.6048E-3		1.4201E-2		2.2006E-1	
1/20	8.8204E-4	2.9046	3.6434E-3	1.9626	1.1176E-1	0.9775
1/40	1.1818E-3	-0.4221	9.2095E-4	1.9841	5.6533E-2	0.9833
1/80	4.6651E-4	1.3410	2.3217E-4	1.9880	2.8513E-2	0.9875
1/160	2.7896E-4	0.7418	5.9441E-5	1.9656	1.4433E-2	0.9822
1/320	1.3096E-4	1.0909	1.5142E-5	1.9729	7.2890E-3	0.9856
1/640	6.5531E-5	0.9989	4.3370E-6	1.8038	3.7437E-3	0.9612
1/1280	3.2230E-5	1.0238	1.5884E-6	1.4491	1.9777E-3	0.9206

Table 3.3: Errors of IFE solutions u_h with $\beta^- = 1$ and $\beta^+ = 10$.

h	$\|\cdot\|_{\infty,\Omega}$	rate	$\|\cdot\|_{0,\Omega}$	rate	$\|\cdot\|_{1,\Omega}$	rate
1/10	3.9354E-3		2.9595E-3		4.6647E-2	
1/20	2.7893E-3	0.4966	1.4801E-3	0.9997	3.2158E-2	0.5366
1/40	1.2467E-3	1.1618	4.7250E-4	1.6473	1.7576E-2	0.8716
1/80	4.5868E-4	1.4425	1.3813E-4	1.7743	9.0342E-3	0.9601
1/160	1.4908E-4	1.6214	3.0164E-5	2.1951	4.4773E-3	1.0128
1/320	3.2708E-5	2.1884	6.6100E-6	2.1901	2.2134E-3	1.0163
1/640	1.2790E-5	1.3546	1.5700E-6	2.0739	1.1073E-3	0.9992
1/1280	3.9359E-6	1.7003	3.7951E-7	2.0485	5.5372E-4	0.9998

Table 3.4: Errors of IFE solutions u_h with $\beta^- = 10$ and $\beta^+ = 10000$.

Chapter 4

Conclusion and Future Work

In this chapter, we first summarize all the results obtained in this thesis and then list a few topics we would like to pursue in the future.

We have developed a new linear immersed finite element(IFE) space according to the actual interface curve for solving the second order elliptic interface problems. We prove the unisolvance of IFE shape functions, i.e., the IFE shape functions can be uniquely determined by their values at the vertices of elements, by showing that the coefficients in an IFE shape function satisfy a Sherman-Morrison linear system. We have presented a group of properties of the constructed IFE shape functions, including the boundedness, partition of unity and the fundamental identities. We derive some geometric identities and estimates about the interface and the straight line connecting the intersection points of the interface with element edges. Based on these geometric estimates and the properties of the IFE shape functions, we have proven that the proposed IFE space has the optimal approximation capability. Also we present numerical experiments that demonstrate the optimal approximation capability as predicted by the related theoretical analysis.

The future work regrading IFE methods include both the error analysis for new schemes and applications to other interface problems.

Error analysis for IFE methods

For the elliptic interface problems, numerical results suggest the IFE solutions based on the partial penalty immersed finite element(PPIFE) methods from [39] have optimal convergence rate for the proposed IFE spaces. According to this observation, it is interesting for us to carry out error analysis for the partial penalty formulation. Another interesting topic is the Petrov Galerkin method in which the standard finite element shape functions are used as the test functions [29].

Applications to other interface problems

We would like to apply the proposed framework on developing and analyzing IFE spaces for elasticity interface problems in the near future. The incompressible Stokes and Navier-Strokes equations will be another interesting topic. Besides, we plan to apply the proposed IFE spaces on solving inverse problems such as the shape optimization problems in which the unknown is the interface between multiple materials in the future.

Bibliography

[1] Slimane Adjerid, Mohamed Ben-Romdhane, and Tao Lin. Higher degree immersed finite element spaces constructed according to the actual interface (submitted, 2016).

[2] Slimane Adjerid, Mohamed Ben-Romdhane, and Tao Lin. Higher degree immersed finite element methods for second-order elliptic interface problems. *Int. J. Numer. Anal. Model.*, 11(3):541–566, 2014.

[3] Slimane Adjerid and Tao Lin. A p-th degree immersed finite element for boundary value problems with discontinuous coefficients. *Appl. Numer. Math.*, 59(6):1303–1321, 2009.

[4] John W. Barrett and Charles M. Elliott. Fitted and unfitted finite-element methods for elliptic equations with smooth interfaces. *IMA J. Numer. Anal.*, 7(3):283–300, 1987.

[5] Z. Belhachmi and H. Meftahi. Shape sensitivity analysis for an interface problem via minimax differentiability. *Applied Mathematics and Computation*, 219(12):6828, 2013.

[6] Dietrich Braess. *Finite elements*. Cambridge University Press, Cambridge, second edition, 2001. Theory, fast solvers, and applications in solid mechanics, Translated from the 1992 German edition by Larry L. Schumaker.

[7] James H. Bramble and J. Thomas King. A finite element method for interface problems in domains with smooth boundaries and interfaces. *Adv. Comput. Math.*, 6(2):109–138, 1996.

[8] Susanne C. Brenner and L. Ridgway Scott. *The mathematical theory of finite element methods*, volume 15 of *Texts in Applied Mathematics*. Springer-Verlag, New York, 1994.

[9] Waixiang Cao, Xu Zhang, and Zhimin Zhang. Superconvergence of immersed finite element methods for interface problems. *Advances in Computational Mathematics*, pages 1–27, 2017.

[10] Chuan Miao Chen. Some estimates for interpolation approximations and their applications. *Numer. Math. J. Chinese Univ.*, 6(1):35–43, 1984.

[11] Zhiming Chen and Jun Zou. Finite element methods and their convergence for elliptic and parabolic interface problems. *Numer. Math.*, 79(2):175–202, 1998.

[12] Eric T. Chung, Tony F. Chan, and Xue-Cheng Tai. Electrical impedance tomography using level set representation and total variational regularization. *Journal of Computational Physics*, 205(1):357–372, 2005.

[13] Philippe G. Ciarlet. *The finite element method for elliptic problems*. North-Holland Publishing Co., Amsterdam-New York-Oxford, 1978. Studies in Mathematics and its Applications, Vol. 4.

[14] Ray W. Clough and James L. Tocher. Finite element stiffness matrices for analysis of plate bending. In *Matrix Methods in Structual Mechanics*, pages 515–545, 1966.

[15] M. Crouzeix and P.-A. Raviart. Conforming and nonconforming finite element methods for solving the stationary Stokes equations. I. *Rev. Française Automat. Informat. Recherche Opérationnelle Sér. Rouge*, 7(R-3):33–75, 1973.

[16] M Giacomini, O Pantz, and K Trabelsi. An a posteriori error estimator for shape optimization: application to eit. *Journal of Physics: Conference Series*, 657(1):012004, 2015.

[17] Yan Gong, Bo Li, and Zhilin Li. Immersed-interface finite-element methods for elliptic interface problems with nonhomogeneous jump conditions. *SIAM J. Numer. Anal.*, 46(1):472–495, 2007/08.

[18] Ruchi Guo and Tao Lin. A group of immersed finite element spaces for elliptic interface problems. *arXiv:1612.01862*, 2016.

[19] Ruchi Guo, Tao Lin, and Xu Zhang. Nonconforming immersed finite element spaces for elliptic interface problems. *arXiv:1612.01862*, 2016.

[20] Johnny Guzmán, Nanuel A. Sánchez, and Marcus Sarkis. A finite element method for high-contrast interface problems with error estimates independent of contrast.

[21] Johnny Guzmán, Nanuel A. Sánchez, and Marcus Sarkis. A finite element method for high-contrast interface problems with error estimates independent of contrast. *arXiv:1507.03873v3*, 2016.

[22] Johnny Guzmán, Nanuel A. Sánchez, and Marcus Sarkis. Higher-order finite element methods for elliptic problems with interfaces. *ESAIM: M2AN*, 50(5):1561–1583, 2016.

[23] Johnny Guzmán, Nanuel A. Sánchez, and Marcus Sarkis. On the accuracy of finite element approximations to a class of interface problems. *Mathematics of Computation*, 85:2071–2098, 2016.

[24] Anita Hansbo and Peter Hansbo. An unfitted finite element method, based on Nitsche's method, for elliptic interface problems. *Comput. Methods Appl. Mech. Engrg.*, 191(47-48):5537–5552, 2002.

[25] Helmut Harbrecht and Johannes Tausch. On the numerical solution of a shape optimization problem for the heat equation. *SIAM Journal on Scientific Computing*, 35(1):A.104–A121, 2013.

[26] Xiaoming He. *Bilinear immersed finite elements for interface problems*. PhD thesis, Virginia Polytechnic Institute and State University, 2009.

[27] Xiaoming He, Tao Lin, and Yanping Lin. Approximation capability of a bilinear immersed finite element space. *Numer. Methods Partial Differential Equations*, 24(5):1265–1300, 2008.

[28] Xiaoming He, Tao Lin, and Yanping Lin. A bilinear immersed finite volume element method for the diffusion equation with discontinuous coefficient. *Commun. Comput. Phys.*, 6(1):185–202, 2009.

[29] Songming Hou and Xu-Dong Liu. A numerical method for solving variable coefficient elliptic equation with interfaces. *Journal of Computational Physics*, 202(2):411–445, 2005.

[30] Jian-Ming Jin. *The finite element method in electromagnetics*. Wiley, New York, 1993.

[31] David A. Kopriva. *Implementing spectral methods for partial differential equations: algorithms for scientists and engineers*. Springer, 2009.

[32] Do Y. Kwak, Kye T. Wee, and Kwang S. Chang. An analysis of a broken P_1-nonconforming finite element method for interface problems. *SIAM J. Numer. Anal.*, 48(6):2117–2134, 2010.

[33] Randall J. LeVeque and Zhi Lin Li. The immersed interface method for elliptic equations with discontinuous coefficients and singular sources. *SIAM J. Numer. Anal.*, 31(4):1019–1044, 1994.

[34] Zhilin Li. The immersed interface method using a finite element formulation. *Appl. Numer. Math.*, 27(3):253–267, 1998.

[35] Zhilin Li and Kazufumi Ito. *The immersed interface method*, volume 33 of *Frontiers in Applied Mathematics*. Society for Industrial and Applied Mathematics (SIAM), Philadelphia, PA, 2006. Numerical solutions of PDEs involving interfaces and irregular domains.

[36] Zhilin Li, Tao Lin, Yanping Lin, and Robert C. Rogers. An immersed finite element space and its approximation capability. *Numer. Methods Partial Differential Equations*, 20(3):338–367, 2004.

[37] Zhilin Li, Tao Lin, and Xiaohui Wu. New Cartesian grid methods for interface problems using the finite element formulation. *Numer. Math.*, 96(1):61–98, 2003.

[38] Tao Lin, Yanping Lin, and Xu Zhang. Partially penalized immersed finite element methods for elliptic interface problems. *SIAM J. Numer. Anal.*, 53(2):1121–1144, 2015.

[39] Tao Lin, Qing Yang, and Xu Zhang. Partially penalized immersed finite element methods for parabolic interface problems. *Numer. Methods Partial Differential Equations*, 2015. in press.

[40] Tao Lin and Xu Zhang. Linear and bilinear immersed finite elements for planar elasticity interface problems. *J. Comput. Appl. Math.*, 236(18):4681–4699, 2012.

[41] Gilles Marck and Yannick Privat. On some shape and topology optimization problems in conductive and convective heat transfers. In M. Papadrakakis, M.G. Karlaftis, and N.D. Lagaros, editors, *OPTI 2014, An International Conference on Engineering and Applied Sciences Optimization*, pages 1640–1657, Kos Island, Greece, June 2014.

[42] Ralf Massjung. An unfitted discontinuous galerkin method applied to elliptic interface problems. *SIAM Journal on Numerical Analysis*, 50(6):3134–3162, 2012.

[43] P Neittaanmäki and D Tiba. Fixed domain approaches in shape optimization problems. *Inverse Problems*, 28(9):093001, 2012.

[44] R. Rannacher and S. Turek. Simple nonconforming quadrilateral Stokes element. *Numer. Methods Partial Differential Equations*, 8(2):97–111, 1992.

[45] Ruchi Guo Slimane Adjerid and Tao Lin. High degree immersed finite element spaces by a least squares method. *Submitted*, 2016.

[46] Carlos F Tolmasky and Andreas Wiegmann. Recovery of small perturbations of an interface for an elliptic inverse problem via linearization. *Inverse Problems*, 15(2):465, 1999.

[47] Fei Wang, Yuanming Xiao, and Jinchao Xu. High-order extended finite element methods for solving interface problems. *arXiv:1604.06171*, 2016.

[48] Jinchao Xu. Estimate of the convergence rate of the finite element solutions to elliptic equation of second order with discontinuous coefficients. *Natural Science Journal of Xiangtan University*, 1:1–5, 1982.

[49] Xu Zhang. *Nonconforming Immersed Finite Element Methods for Interface Problems*. 2013. Thesis (Ph.D.)–Virginia Polytechnic Institute and State University.

[50] Xu Zhang. Nonconforming immersed finite element methods for interface problems. 2013.

[51] Yongcun Zhang and Shutian Liu. The optimization model of the heat conduction structure. *Progress in Natural Science*, 18(6):665 – 670, 2008.